Title: Refractory for Black Liquor Gasifiers

Type of Report: Quarterly Report

Reporting Period Start Date: April 1, 2004

Reporting Period End Date: June 30, 2004

Principal Authors: William L. Headrick Jr., Musa Karakus, Xiaoting Liang and Alireza Rezaie

Date Report Issued: July 2004

DOE Award Number: DE-FC26-02NT41491

Name and Address of Submitting Organization:
Curators of the University of Missouri on behalf of University of Missouri-Rolla
Sponsored Programs
1870 Miner Circle
215 ME Annex
Rolla, MO 65409-1330

DISCLAIMER

ABSTRACT

The University of Missouri-Rolla will identify materials that will permit the safe, reliable and economical operation of combined cycle gasifiers by the pulp and paper industry. The primary emphasis of this project will be to resolve the material problems encountered during the operation of low-pressure high-temperature (LPHT) and low-pressure low-temperature (LPLT) gasifiers while simultaneously understanding the materials barriers to the successful demonstration of high-pressure high-temperature (HPHT) black liquor gasifiers. This study will define the chemical, thermal and physical conditions in current and proposed gasifier designs and then modify existing materials and develop new materials to successfully meet the formidable material challenges. Resolving the material challenges of black liquor gasification combined cycle technology will provide energy, environmental, and economic benefits that include higher thermal efficiencies, up to three times greater electrical output per unit of fuel, and lower emissions. In the near term, adoption of this technology will allow the pulp and paper industry greater capital effectiveness and flexibility, as gasifiers are added to increase mill capacity. In the long term, combined-cycle gasification will lessen the industry's environmental impact while increasing its potential for energy production, allowing the production of all the mill's heat and power needs along with surplus electricity being returned to the grid. An added benefit will be the potential elimination of the possibility of smelt-water explosions, which constitute an important safety concern wherever conventional Tomlinson recovery boilers are operated.

Developing cost-effective materials with improved performance in gasifier environments may be the best answer to the material challenges presented by black liquor gasification. Refractory materials may be selected/developed that either react with the gasifier environment to form protective surfaces in-situ; are functionally-graded to give the best combination of thermal, mechanical, and physical properties and chemical stability; or are relatively inexpensive, reliable repair materials. Material development will be divided into 2 tasks:

Task 1, Development and property determinations of improved and existing refractory systems for black liquor containment. Refractory systems of interest include magnesium aluminate and barium aluminate for binder materials, both dry and hydratable, and materials with high alumina contents, 85-95 wt%, aluminum oxide, 5.0-15.0 wt%, and BaO, SrO, CaO, ZrO_2 and SiC.

Task 2, Finite element analysis of heat flow and thermal stress/strain in the refractory lining and steel shell of existing and proposed vessel designs. Stress and strain due to thermal and chemical expansion has been observed to be detrimental to the lifespan of existing black liquor gasifiers. The thermal and chemical strain as well as corrosion rates must be accounted for in order to predict the lifetime of the gasifier containment materials.

TABLE OF CONTENTS

LIST OF GRAPHICAL MATERIALS

INTRODUCTION

Worldwide growth of black liquor production as a new source of energy and electricity necessitates the development of new refractory materials resistant to harsh operating conditions of black liquor gasifiers. Black liquor is a by-product of the papermaking process. Black liquor is an aqueous solution containing waste organic material, which is mainly lignin, as well as the spent pulping chemicals, which are primarily sodium carbonate and sodium sulfide [1]. Chemical energy can be recovered from black liquor by burning it as a liquid fuel in a boiler or gasifier [1, 2]. Black Liquor Gasification (BLG) is widely viewed as the technology that will replace the recovery boiler in the pulp and paper industry [3]. Similar gasification processes are used to convert low-cost solids such as biomass or waste liquids into clean-burning gases [3]. Combustion of these gases has the potential to partially or fully meet the energy needs for pulp and paper plants, reducing or eliminating dependence on electricity generated commercially by the combustion of fossil fuels [4]. The fundamentals of the gasification process have been reviewed elsewhere [4]. The scope of this project will be on high temperature process (900-1000ºC) developed by Chemrec [5]. The operating conditions of the process were studied in Task 1.0 and thermodynamic analysis was performed based upon the results of this study.

Thermodynamics based on chemical analysis showed that the composition of black liquor smelt that would contact the refractory lining is 70-75% Na_2CO_3 (T_m=858°C), 20-25% Na_2S (T_m=1172°C) and 2-5% K_2CO_3 (T_m=901°C). To date, aluminosilicate or fused cast alumina-based materials have been used in this application. Both thermodynamic calculations and experience show that these aluminosilicates are not sufficiently resistant to the alkali containing atmospheres for extended operation of gasifiers. Thermodynamic analysis showed that oxides such as magnesia, ceria and zirconia or aluminates such as barium and lithium aluminate may have satisfactory stability against black liquor smelt. Non-oxides such as SiC and Si_3N_4 were dissolved by black liquor smelt and were not candidates for this application. The objective of task 1.2 was to verify the results of thermodynamics by experiments.

A nonlinear finite element model was created for the Chemrec type gasifier reactor to simulate the operational thermomechanical environment in Task 2.0. The heat transfer and thermomechnical results were given for the understanding of the behavior of refractory material during operational conditions.

EXECUTIVE SUMMARY

Black liquor gasification is a high potential technology for production of energy which allows substitution for other sources of energy. This process uses a waste of the pulp and paper industry as black liquor to produce synthetic gas and steam for production of electricity; therefore development of this technology not only recovers the waste of the paper industry but also decreases dependency on fossil fuel.

Today one of the main obstacles in the development of this technology is the development of refractory materials for protective lining of the gasifier. So far the materials used for this application have been based on alumino-silicate refractories but, thermodynamics and experience shows that these materials are not sufficiently resistant to black liquor under the harsh working conditions of Black liquor gasifiers. Consequently development of cost-effective materials with improved performance in gasifier environments to answer the material challenges presented by black liquor gasification (HTHP, HTLP) is the objective of this project.

FactSage® thermodynamic modeling software can convert the elemental analysis composition of the black liquor to compound composition. This results show that at 950ºC, black liquor smelt flowing on the refractory lining installed on the gasifier vessel shell is composed of 70-75% sodium carbonate, 20-25% sodium sulfide and 2-5% potassium carbonate. Sodium and potassium carbonate are molten at 950ºC while sodium sulfide is in solid state if it is assumed that there is no solution between sodium sulfide and carbonates. Obviously, the selection of refractory materials for this application should be based upon resistance to molten Na_2CO_3 although Na_2S and K_2CO_3 should not be ignored.

Thermodynamic data shows that none of refractory compounds in the alumino-silicate system are resistant to black liquor. At 950ºC , corundum converts to β"-alumina, β-alumina and K-β-alumina while mullite converts to nepheline, albite, leucite and corundum in contact with Black Liquor. All these phase transformations are associated with large volume expansion. Also thermodynamic data shows that simple oxides including ZrO_2, CeO_2, La_2O_3, Y_2O_3, Li_2O, MgO and CaO are resistant to black liquor but non-oxides such as SiC and Si_3N_4 are oxidized and dissolved in black liquor. Ellingham diagram presents us with the fact that all candidate refractory simple oxides are resistant to both sodium and potassium metal vapors at operating temperature of BLG and none of them are reduced to metallic form.

The other candidates for BLG application are aluminates including $MgAl_2O_4$, $BaAl_2O_4$ and $LiAlO_2$. FactSage database showed that none of the aluminates were resistant to sodium oxide in the range of operating temperature of high temperature black liquor gasifier although all three are resistant to sodium carbonate. They form $NaAlO_2$ in contact with sodium oxide. It was observed that none of the aluminates were resistant to potassium oxide and potassium carbonate except lithium aluminate which was stable with potassium carbonate. The reaction product of aluminates with potassium oxide or carbonate was $KAlO_2$.

A nonlinear finite element model was created for the Chemrec type gasifier reactor to simulate the operational thermomechanical environment. The heat transfer and thermomechnical results were given for the understanding of the behavior of refractory material during operational conditions.

EXPERIMENTAL

Sessile drop testing was employed to measure the contact angle between the candidate refractory materials and black liquor components. The thermodynamics of interaction of the materials with black liquor smelt was studied before [6]. The schematic of the equipment used for sessile drop testing is presented in Figure 1. The system was designed for the precise determination of the contact angle of liquid droplets on solid substrates under controlled conditions of temperature and atmosphere. The main features of the system are the sessile drop furnace, the controlled atmosphere and the image acquisition system. The furnace was a horizontal tube furnace, resistant heated with Ni-chrome wire with a high-purity, dense and impermeable mullite reaction tube. Each candidate material substrate was placed on an alumina D-tube which was positioned at the center at the hot zone. The experiments were carried out in argon atmosphere. Sample temperature was controlled to within ±5°C as measured with a K-type thermocouple. An optical-quality, fused quartz window permitted observation of the in-situ sessile drop and video recording of the interface interaction behavior between the substrate and the smelt.

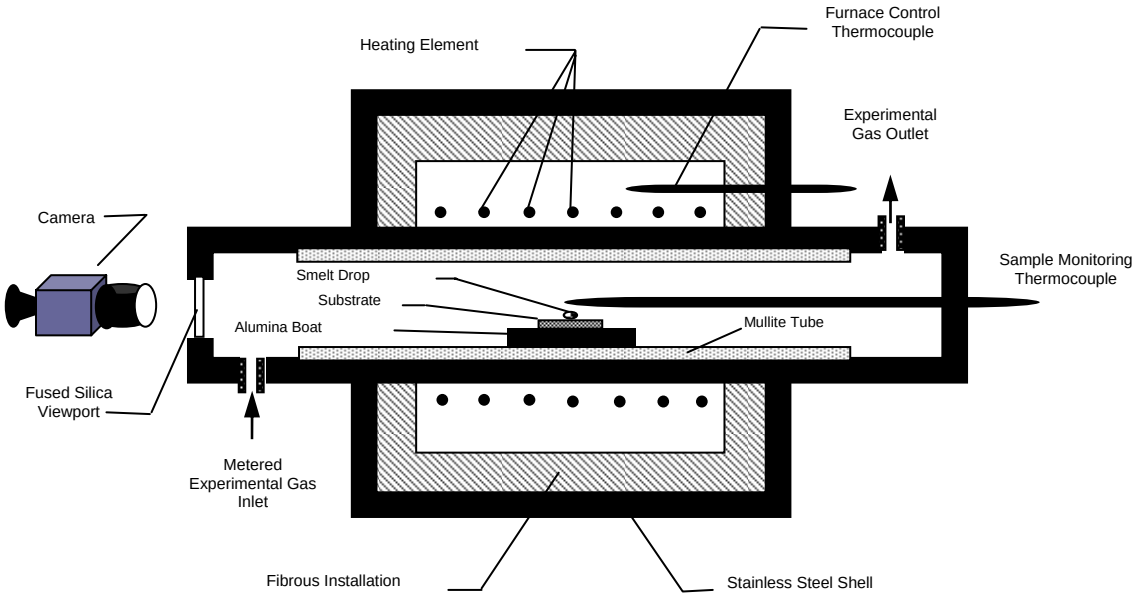

Figure 1: Sessile drop test equipment to measure the contact angle

In sessile drop experiments, smelt powder (0.2-0.3 g), sodium carbonate and potassium carbonate, was formed into 1/4" diameter cylindrical geometry by uniaxial pressing using a 1/4" stainless steel die. The formed smelt powder was placed on the substrate and the liquid drop was formed by heating the drop to 1000°C in 2.5 hours and maintained at 1000°C for 10 hours. Long soaking time was selected to overcome the kinetic barrier and let the sample react with the smelt if there was no thermodynamic barrier. The image of the sessile drop was recorded by a camera and the contact angle was measured at the temperature of complete melting of the drop using enlargement of a photograph extracted from recorded video film of entire test. The average of the 5-7 values was taken as the contact angle.

After cooling from the final sessile drop test temperature (1000°C), the interaction between the solidified smelt and the substrate was examined by thin film x-ray diffraction. If the results of thin film analysis were not satisfactory, the mixture of the powder of each candidate with smelt powder was heated to 1000°C under the same conditions as the sessile drop test. The reaction products were ground to "-200" mesh powder and analyzed by x-ray diffraction. The interface was also examined in a scanning electron microscope (SEM; Hitachi S-570) and with energy dispersive x-ray analysis by sectioning the substrate across the interface but it was not possible to determine the depth of reaction with scanning electron microscopy, as the contrast between the original oxides and the reaction products was not high enough to accurately estimate a reaction depth. In addition, energy dispersive spectrometry could not adequately detect sodium, a relatively light element close to the detection limit of the apparatus. Moreover, because sessile drop test is not an appropriate test to do kinetic studies on corrosion and compare the resistance of different materials, a simulative corrosion test such as finger test will be used to study the resistance of different materials to react with black liquor. If x-ray diffraction analysis doesn't show any reaction of the material with black liquor or the constituents, kinetic studies of the reaction do not seem meaningful. In this case, only microstructural features such as porosity, grain size or impurity will affect the corrosion kinetics.

The substrates of Al_2O_3, MgO and CeO_2 candidate materials were formed in 3/4" diameter and 0.2-0.4" height of high purity powder (>99.5%) , sintered at 1600°C for 2 hours to get to about 95% of the theoretical density with almost no open porosity. The substrates of mullite ($3Al_2O_3.2SiO_2$), Y_2O_3, ZrO_2, $MgAl_2O_4$, $LiAlO_2$ and $BaAl_2O_4$ were fabricated in cylindrical shape with 1.5" diameter and 0.1-0.2" height to obtain 97% of theoretical density and no open porosity. The surface of each substrate was ground using sand paper and then polished with diamond paste down to 1μm to form a smooth surface required to measure the contact angle. The open porosity and the density (relative to theoretical density) of each substrate measured by Archimedes method is reported in Figure 2 and 3.

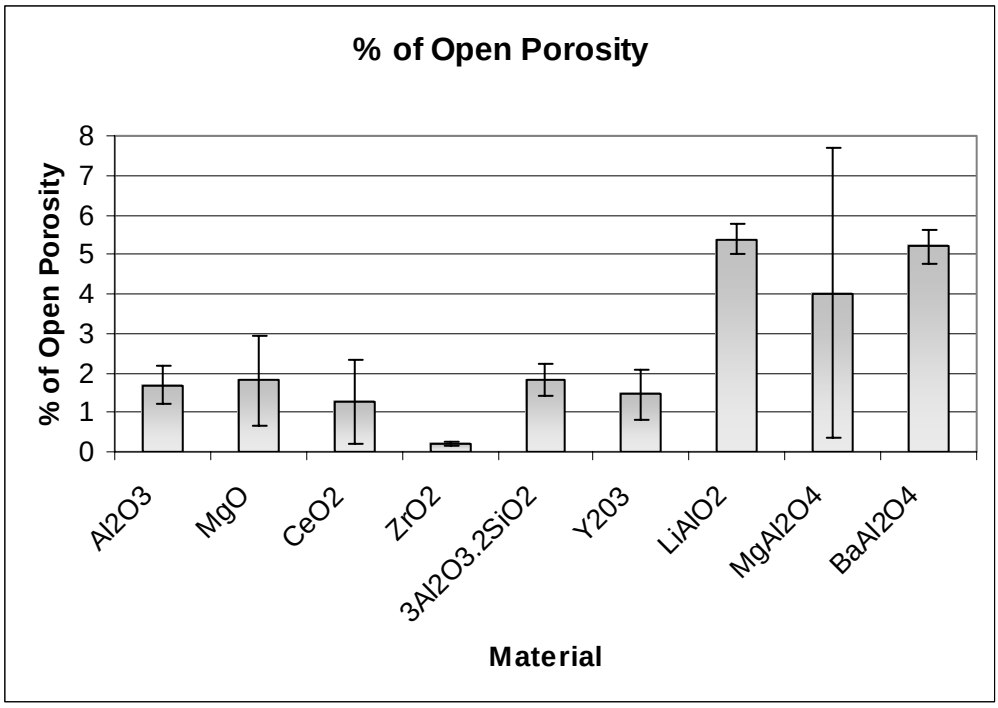

Figure 2: % of open porosity of the substrates used in sessile drop testing

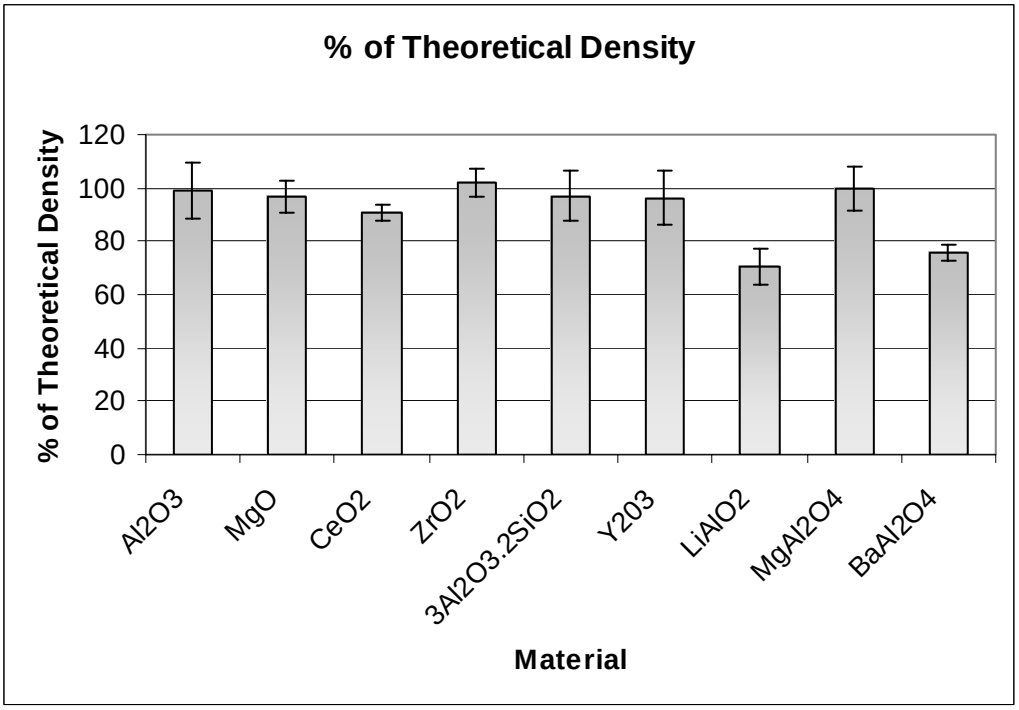

Figure 3: % of theoretical density of the substrates used in sessile drop test

Among different selected materials, only $LiAlO_2$, $BaAl_2O_4$ and CeO_2 didn't have satisfactory density. But when the % of open porosity is also considered and compared with the % of theoretical density, it is concluded that most of the porosity of the specimen

were closed porosity which wouldn't have considerable effect on the results of sessile drop testing.

RESULTS AND DISCUSSION

Task 1.2

Figure 4 shows a schematic of smelt/specimen interface and measurement of the contact angle. The part of the substrate used to be analyzed by x-ray diffraction and studied by SEM is shown as well.

Figure 5 shows the x-ray diffraction pattern of the commercial black liquor supplied by the Weyerhaeuser BLG plant in North Carolina. This pattern verified the results of thermodynamics and showed that black liquor smelt is mainly composed of sodium carbonate and sodium sulfide. Potassium carbonate was not definitely detected due to either insufficient amount in the composition or background noise in the pattern. Sodium oxide in another phase which may exist in black liquor smelt. The other phase that may match the peaks of pattern obtained from the black liquor smelt is sulfur oxide graphite (C_2SO_3) which was not expected by thermodynamics; however, many peaks were unidentified.

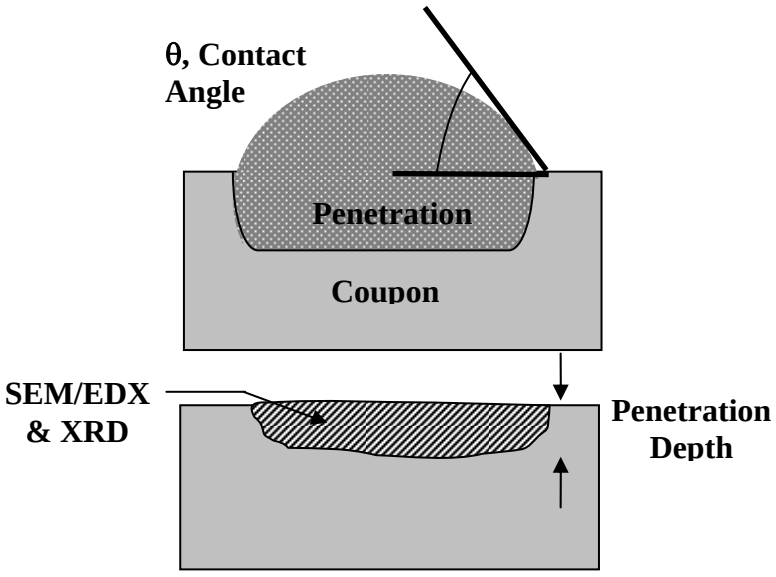

Figure 4: Schematic of contact angle measurement and part of sample analyzed by XRD and SEM/EDX

Sessile drop testing was accomplished with sodium carbonate and potassium carbonate since they are in liquid state at operating temperature of black liquor gasification but sodium sulfide is not.

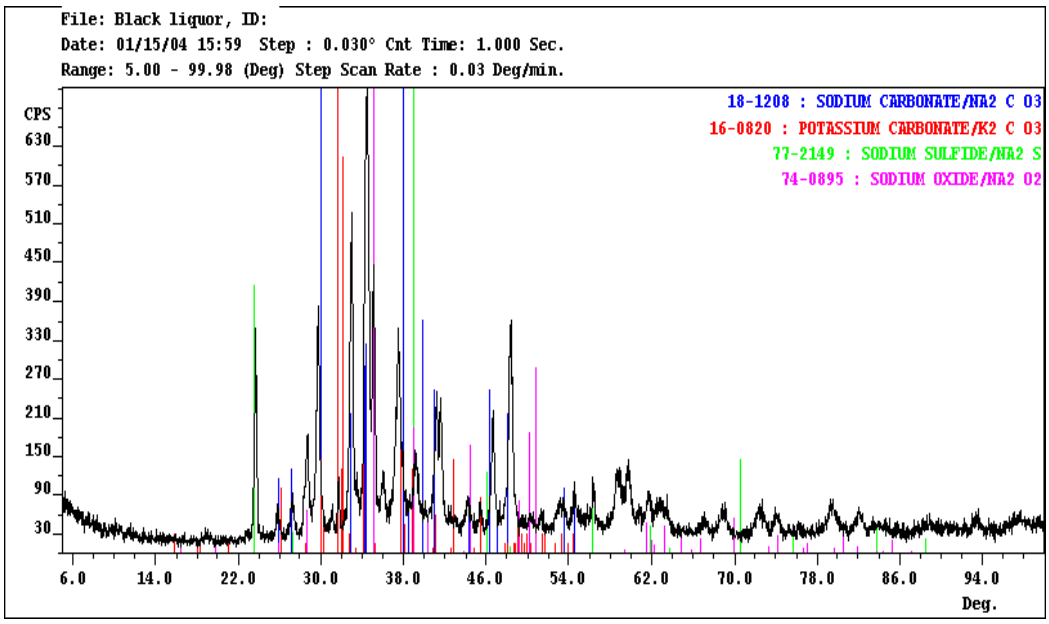

Figure 5: X-ray pattern of black liquor smelt

Figure 6 is a presentation of measured contact angle between the candidate materials and sodium carbonate under argon atmosphere at 1000°C. $MgAl_2O_4$ (spinel) specimen had the highest contact angle (13 ± 1 degrees), but it was still wet by the sodium carbonate. It was expected that the sodium carbonate would wet all oxide refractories. Figure 7 shows Na_2CO_3 drop on spinel substrate at the time it was completely molten and when the measurement was accomplished. Figure 8 shows Na_2CO_3 drop on mullite substrate under the same conditions. The difference of wetting behavior of spinel and mullite with Na_2CO_3 is considerable and distinguishable clearly. Lithium aluminate specimen cracked during sessile drop testing probably due penetration of sodium carbonate through grain boundaries and reaction with the specimen. Results of x-ray diffraction of a powder mixture of lithium aluminate and sodium carbonate at 1000°C under argon atmosphere showed no reaction which is in contradiction with the results of x-ray diffraction obtained from the surface of lithium aluminate disc exposed to sodium carbonate melt in sessile drop testing. Formation of sodium aluminate and specific volume increase of new compound compared to the original phase resulted in the formation of crack in the structure of the material and failure of the specimen. Measurement of contact angle of lithium aluminate with sodium carbonate melt was not possible due to early reaction of the substrate with the melt and crack formation. Formation of crack specifically in grain boundaries is presented in figure 9, 10 and 11. The grain edge areas or the areas close to the grain boundaries with brighter phase shows more sodium in the composition compared to the grain compositions. The qualitative EDS technique verifies the formation of sodium containing phases close to grain boundaries compared to grain composition (Figure 12 and 13). Sodium can either form sodium aluminate or can be dissolved in lithium aluminate and form a solid solution.

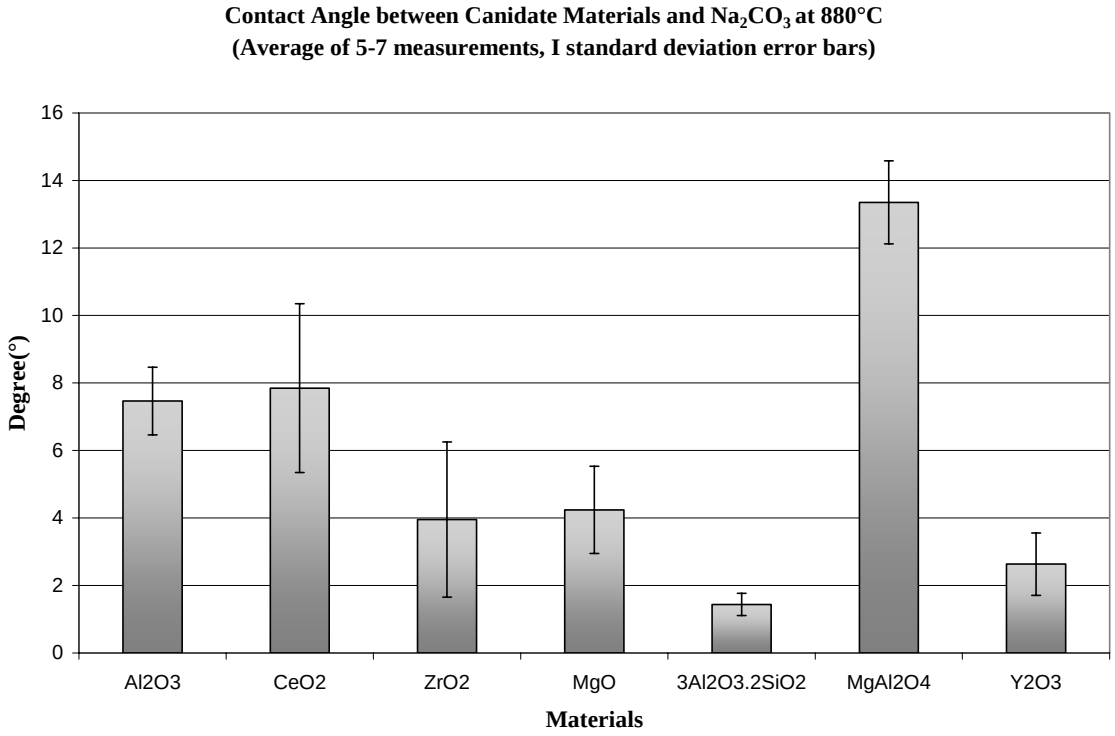

Figure 6: Contact Angle of Na_2CO_3 on dense candidate materials

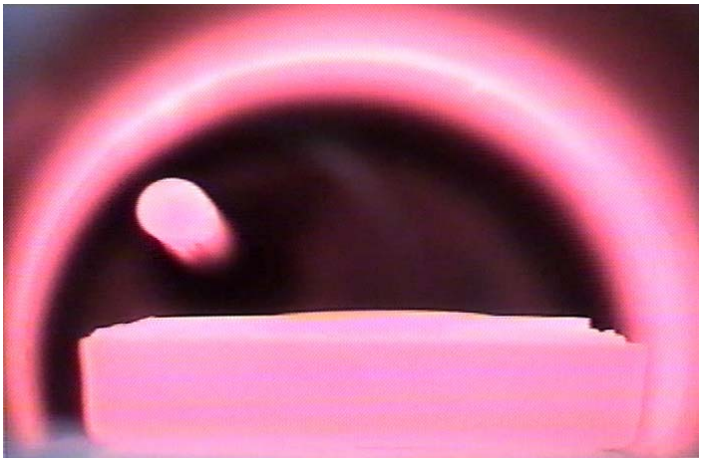

Figure 7: Na_2CO_3 drop on $MgAl_2O_4$ specimen after melting

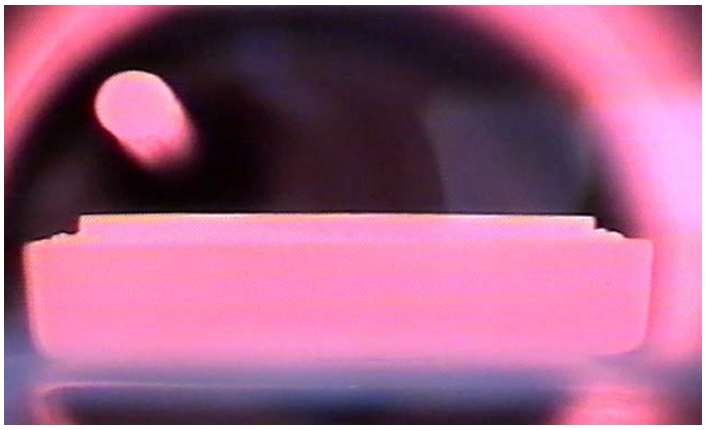

Figure 8: Na_2CO_3 drop on mullite specimen after melting

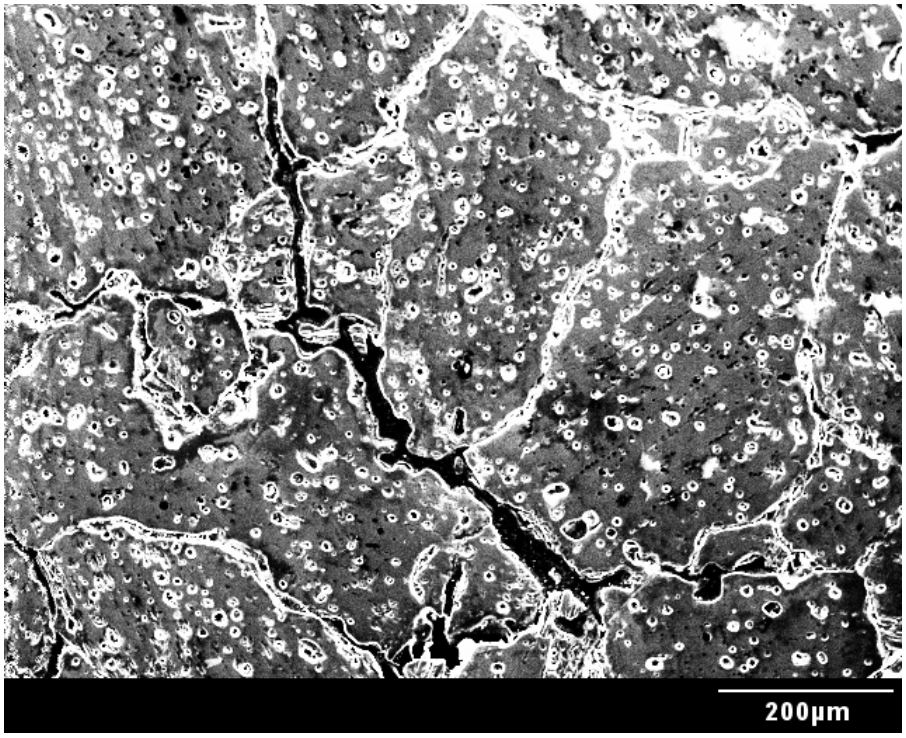

Figure 9: Formation of crack in $LiAlO_2$ substrate due to interaction with sodium carbonate melt (X100/SE/15KV)

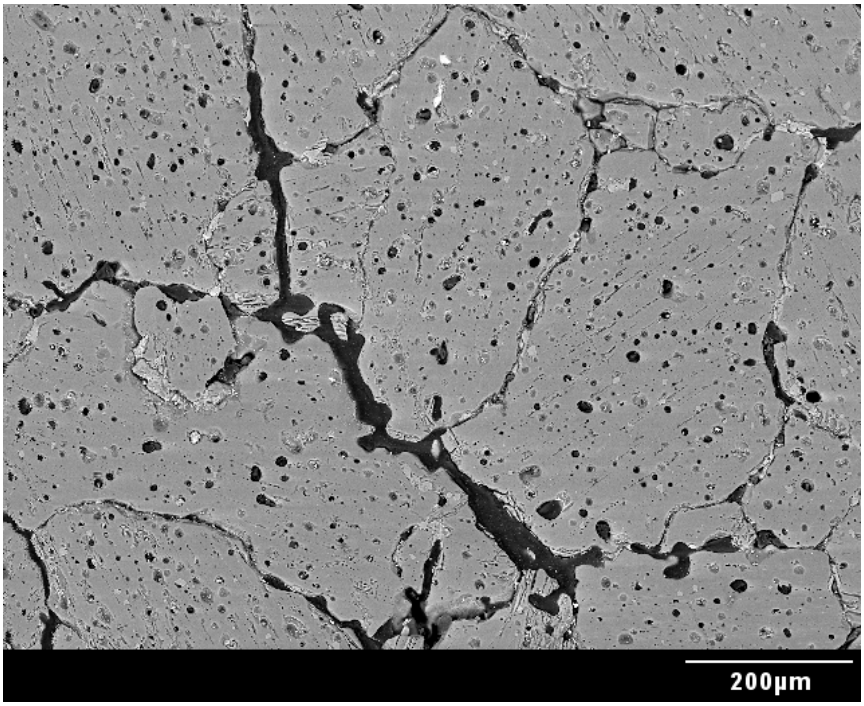

Figure 10: Formation of crack in $LiAlO_2$ substrate due to interaction with sodium carbonate melt (X100/BSE/20KV)

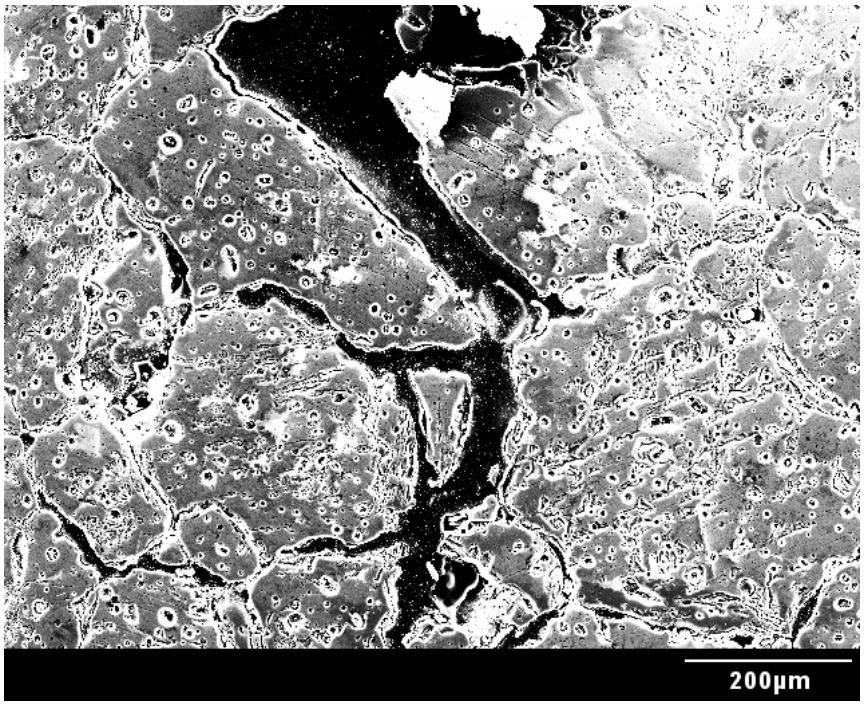

Figure 11: Formation of crack in $LiAlO_2$ substrate due to interaction with sodium carbonate melt (X100/SE/20KV)

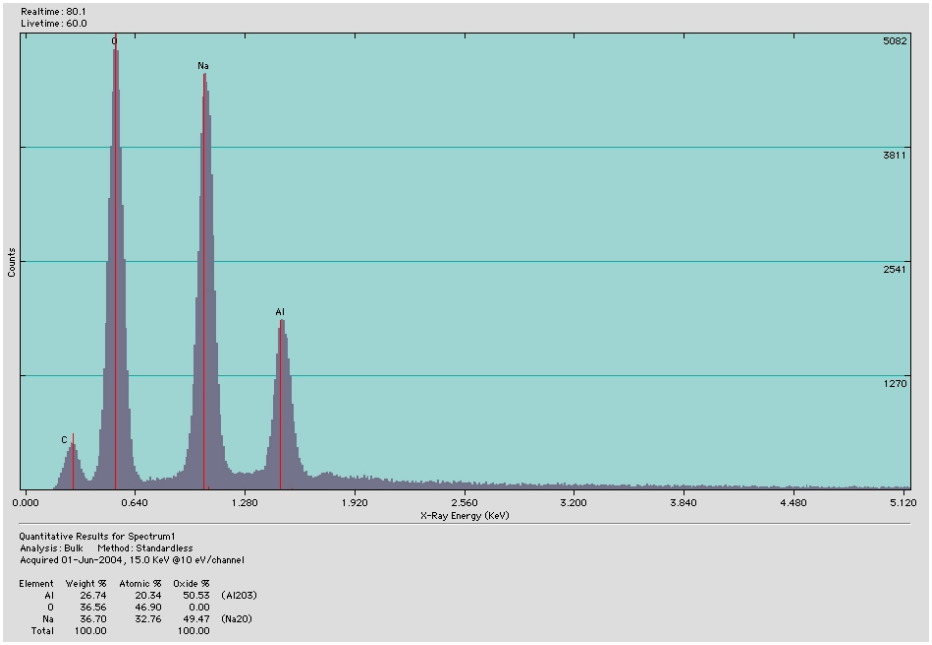

Figure 12: Detection of considerable amount sodium in the areas close to grain boundaries in $LiAlO_2$ substrate

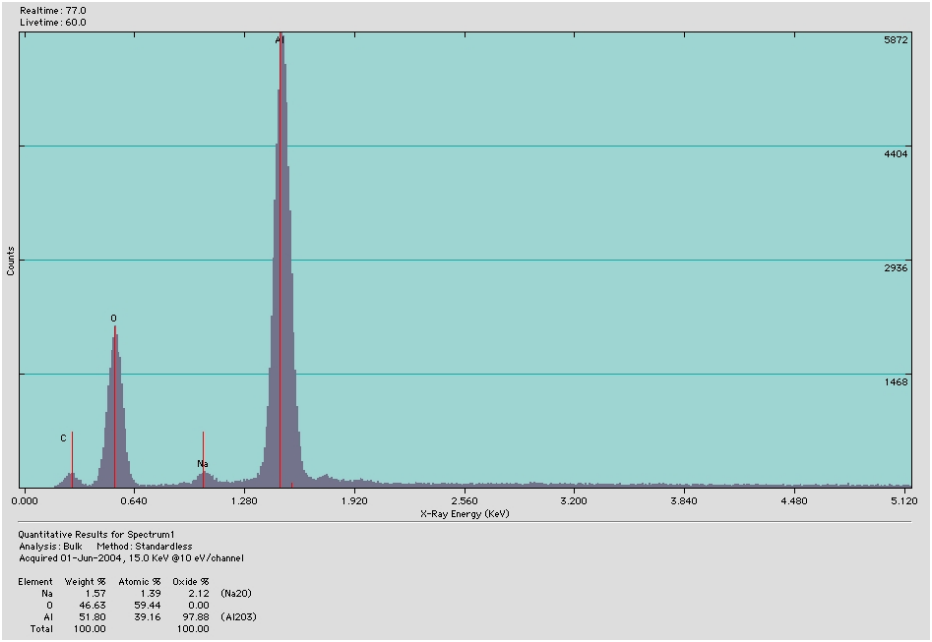

Figure 13: Detection of small amount sodium in grains in $LiAlO_2$ substrate

Formation of cracks in mullite specimen, one of the materials not resistant to sodium carbonate, in the region of the reaction with sodium carbonate was observed as well (Figure 14).

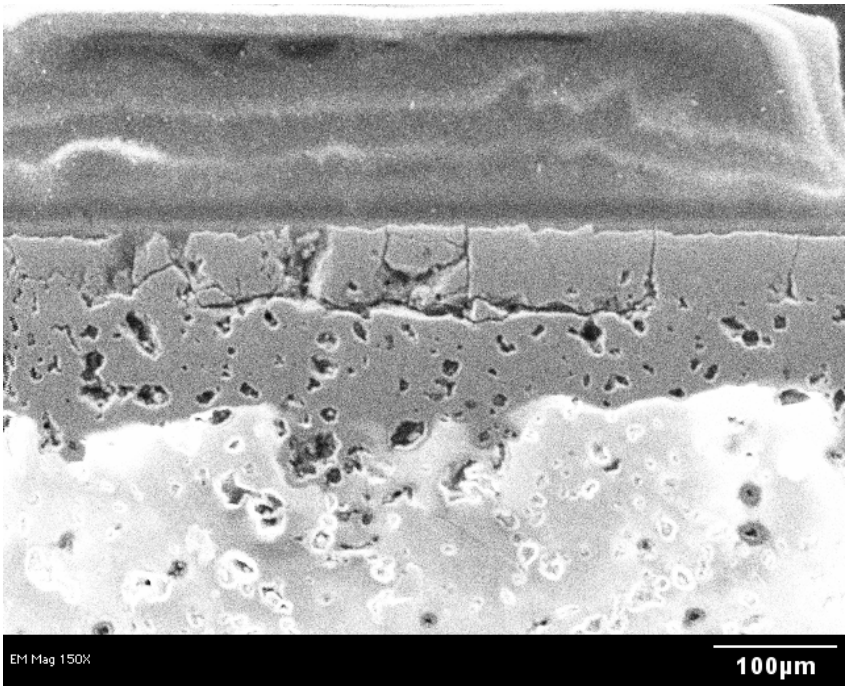

Figure 14: Formation of crack in mullite substrate due to interaction with sodium carbonate melt (X150/BSE/20KV)

Figure 15 is a plot of contact angle between the candidate oxides and potassium carbonate measured to date. In this case magnesium oxide showed the highest wetting angle of about 10 ± 2 degrees.

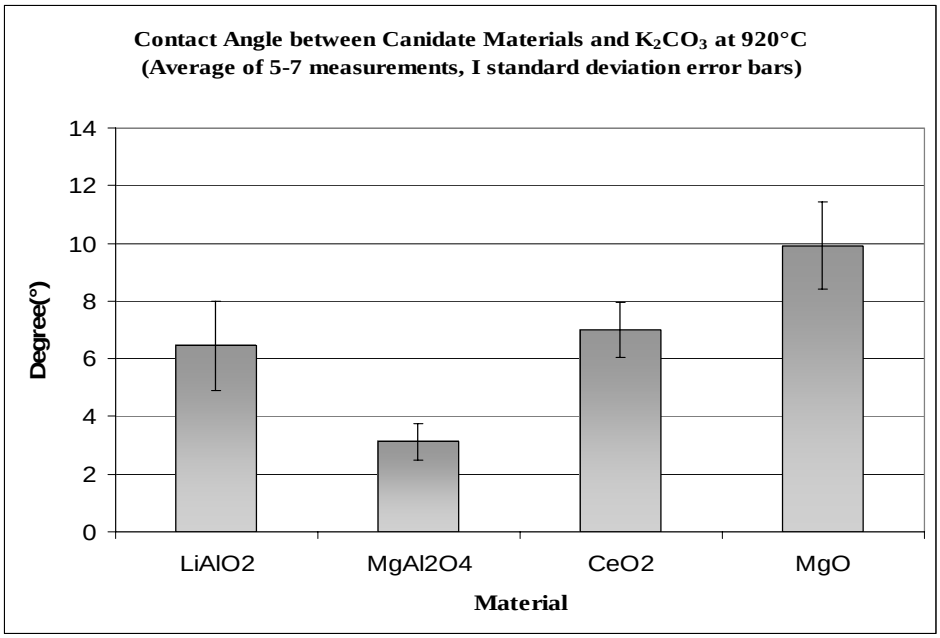

Figure 15: Contact Angle of K_2CO_3 on dense candidate materials

X-ray diffraction was used to determine the reaction products. The depth of beam penetration was varied by controlling the angle of incidence. A low angle of incidence was used to show that the surface coating was indeed sodium carbonate. The surface coating was sodium carbonate for the specimens that did not react. Increasing the angle of incidence increased surface penetration showing sodium carbonate, the original oxide and any reaction products. In some cases it was possible to further increase the angle of incidence to show the original oxide below the reaction zone
Figure 16 shows the formation of reaction product and sodium aluminate between sodium carbonate and alumina as predicted by Fact Sage®. Figure 17 shows the formation of reaction product and sodium aluminum silicate between sodium carbonate and mullite as predicted. Formation of sodium zirconate which was not predicted by Fact Sage® but predicted by Yamaguchi [12] due to reaction between zirconia and sodium carbonate was observed as shown in Figure 18. Figures 19 and 20 show the lack of reaction products with magnesia and ceria as predicted by FactSage®. Figure 21 shows that yttrium oxide in contact with sodium carbonate formed sodium yttrium oxide which Fact Sage® didn't predict. It is observed in Figure 22 that magnesium aluminate spinel precipitated magnesium oxide and formed sodium aluminate in contact with sodium carbonate which is not in agreement with thermodynamic predictions. It seems that the kinetics of reaction is slow between spinel and sodium carbonate at 1000°C because the reaction layer at the surface of the substrate after sessile drop testing was very thin and a relatively thick transparent layer of sodium carbonate smelt had solidified at the surface. X-ray diffraction did not show any reaction between lithium aluminate and sodium carbonate in a powder mixture of the components which agrees with the thermodynamics (Figure 23) but x-ray diffraction from surface of the substrate exposed to sodium carbonate in sessile drop testing shows the formation of sodium aluminate as a new compound (Figure 24). Barium aluminate formed barium carbonate and sodium aluminum oxide in powder

mixtures (Figure 25) at 1000°C under argon. It is predicted that barium aluminate dissociated to barium carbonate and aluminum oxide as the first step and then sodium carbonate reacted with aluminum oxide and formed sodium aluminate.
The materials which didn't show any reaction with sodium carbonate or were among the promising candidates were also tested with potassium carbonate to measure the contact angle and evaluate their reactivity to potassium carbonate. The results showed that both magnesium oxide and cerium oxide were resistant to potassium carbonate as they were resistant to sodium carbonate (Figure 26 and 27) which verified the results of thermodynamic studies. Magnesium aluminate spinel reacted with potassium carbonate and formed magnesium oxide and potassium aluminum oxide as reaction products (Figure 28). Therefore spinel was probably dissociated to magnesium oxide and aluminum oxide first and the reaction between aluminum oxide and potassium carbonate formed potassium aluminate. Also thermodynamics showed that spinel would not be resistant to potassium carbonate. Both lithium aluminate and barium aluminate in powder mixture with potassium carbonate showed no reaction with potassium carbonate as was predicted by Factsage® (Figure 29 and 30) but lithium aluminate substrate exposed to potassium carbonate in sessile drop testing shows some peaks which can be identified as the peaks of potassium aluminate but the formation of new phase cannot be assured (Figure 31).

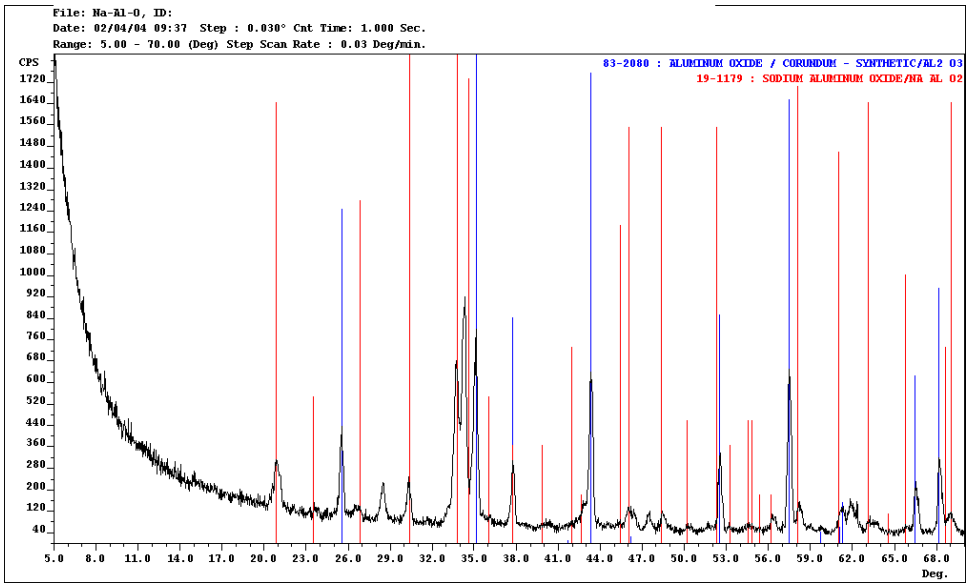

Figure 16: X-ray diffraction pattern showing reaction product sodium aluminate and original corundum

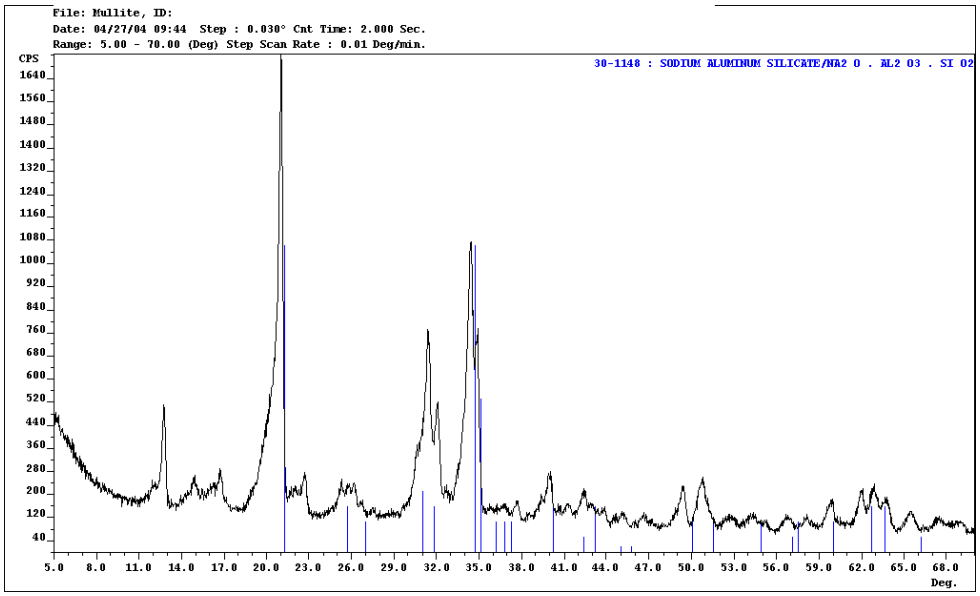

Figure 17: X-ray diffraction pattern showing reaction product sodium aluminum silicate in mullite specimen

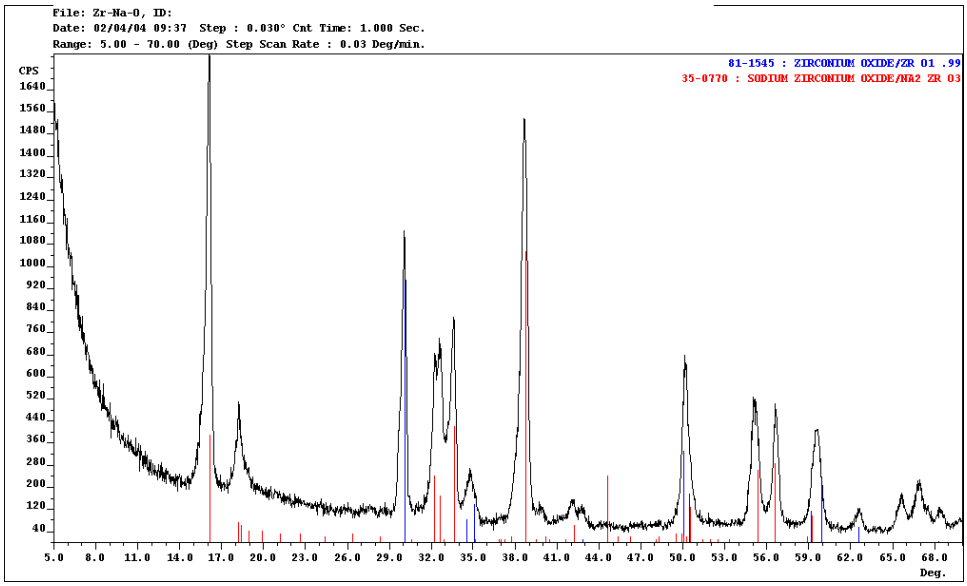

Figure 18: X-ray diffraction pattern showing reaction product sodium zirconium oxide and original zirconia

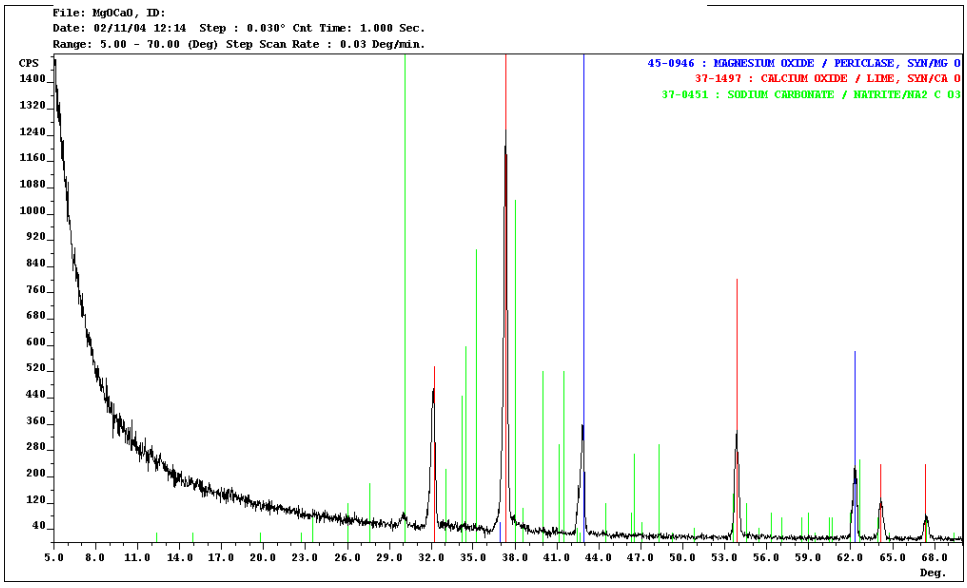

Figure 19: X-ray diffraction pattern showing lack of reaction product with original magnesia, calcia and Na_2CO_3

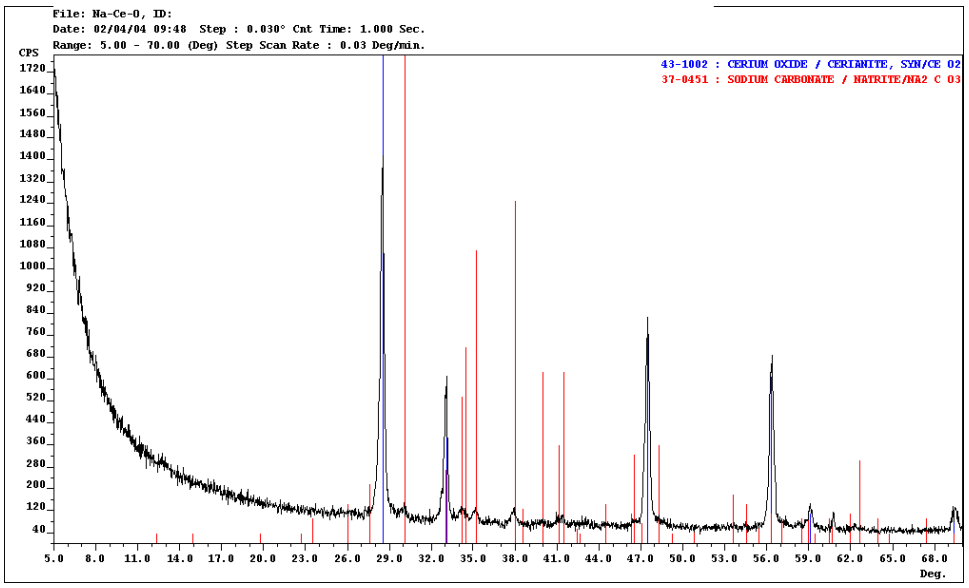

Figure 20: X-ray diffraction pattern showing lack of reaction product with original ceria and Na_2CO_3

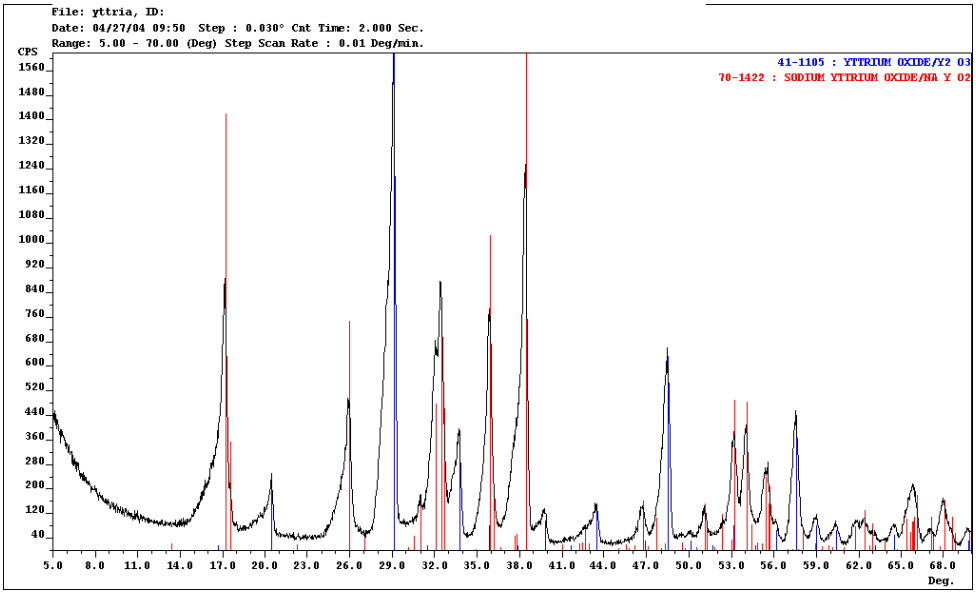

Figure 21: X-ray diffraction pattern showing reaction product sodium yttrium oxide and original yttrium oxide

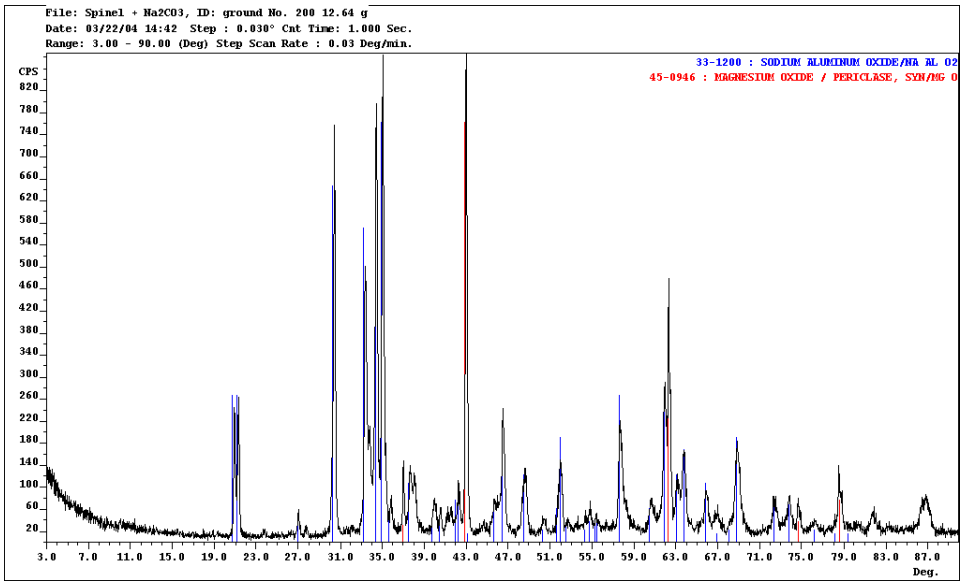

Figure 22: X-ray diffraction pattern showing reaction products sodium aluminum oxide and magnesium oxide in spinel specimen

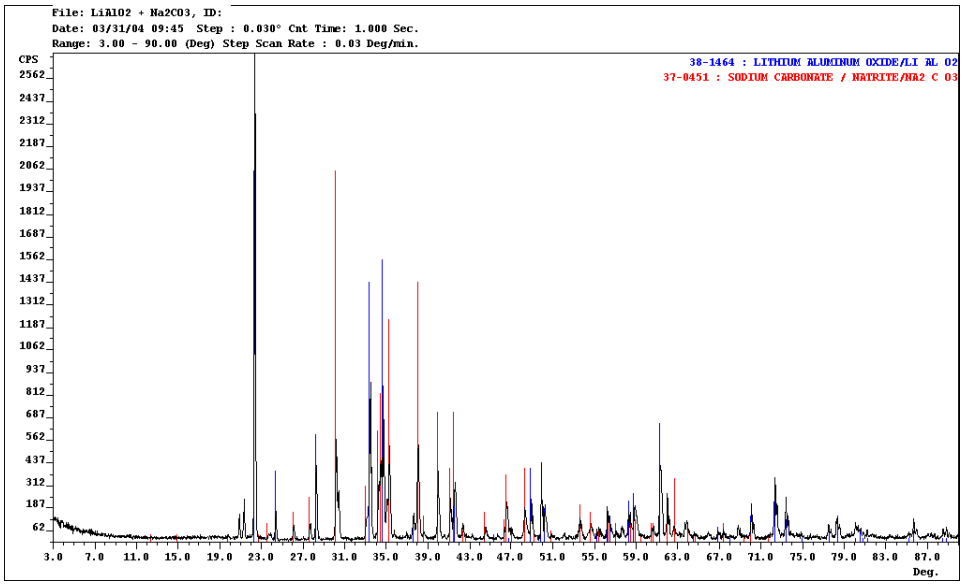

Figure 23: X-ray diffraction pattern showing lack of reaction product with original lithium aluminate and Na_2CO_3 (powder mixture)

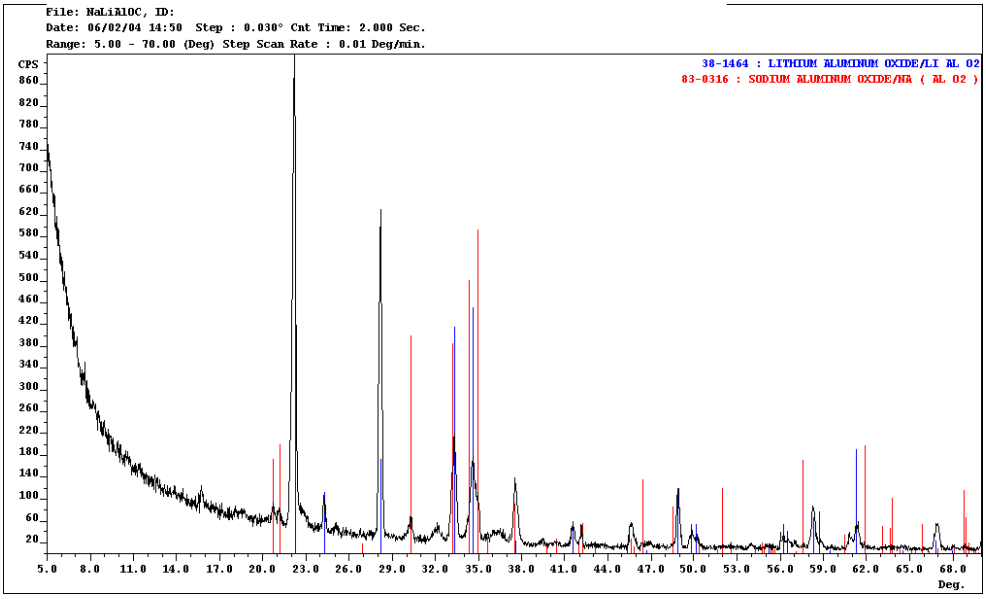

Figure 24: X-ray diffraction pattern showing reaction product of sodium aluminate with original lithium aluminate (Sessile drop testing substrate)

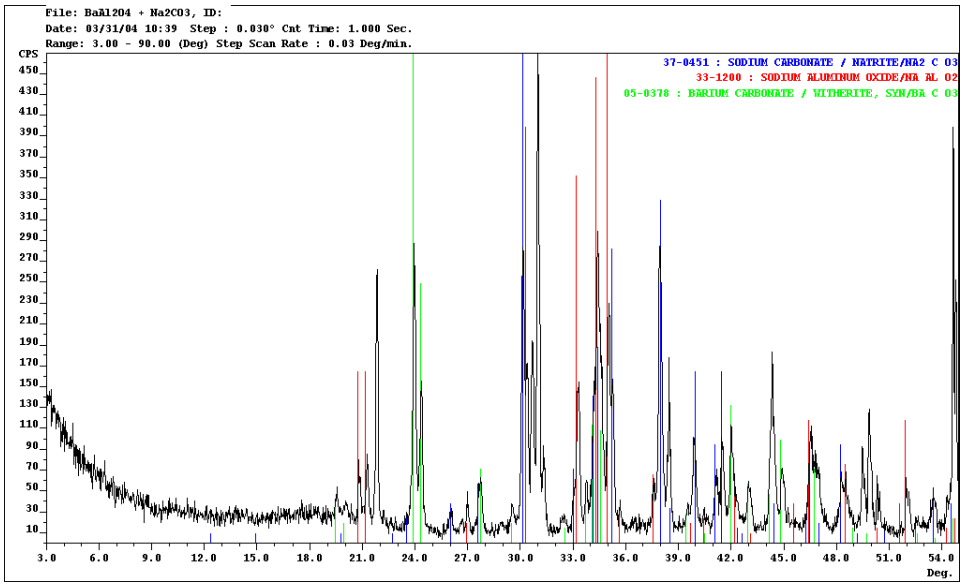

Figure 25: X-ray diffraction pattern showing reaction products of sodium aluminum oxide, barium carbonate and original Na_2CO_3 smelt (powder mixture)

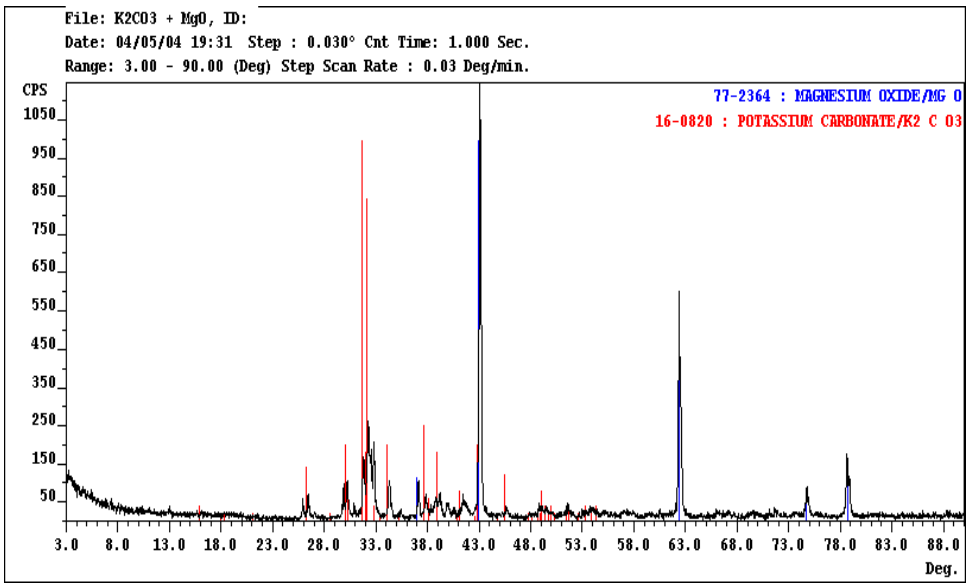

Figure 26: X-ray diffraction pattern showing lack of reaction product with original magnesium oxide and K_2CO_3

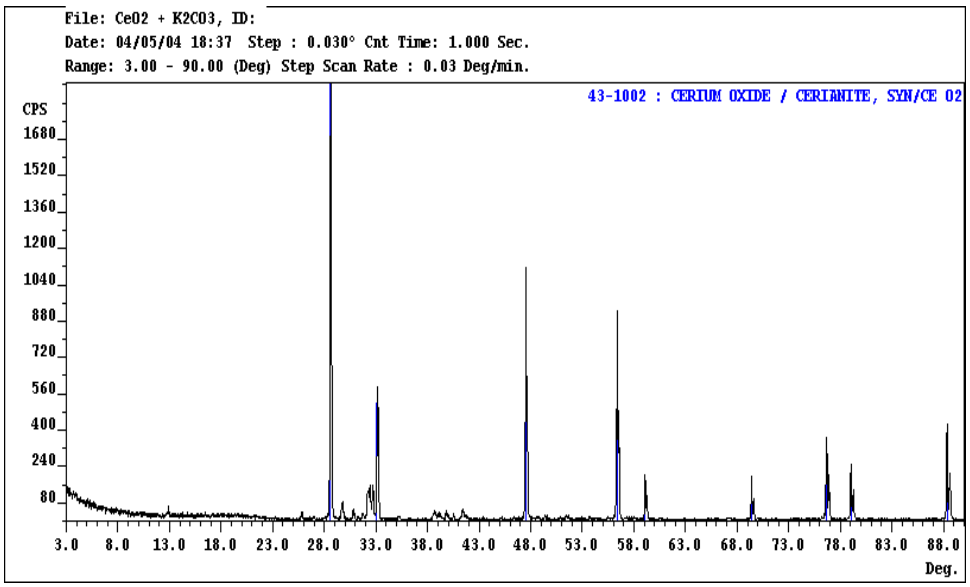

Figure 27: X-ray diffraction pattern showing lack of reaction product with original cerium oxide and K_2CO_3

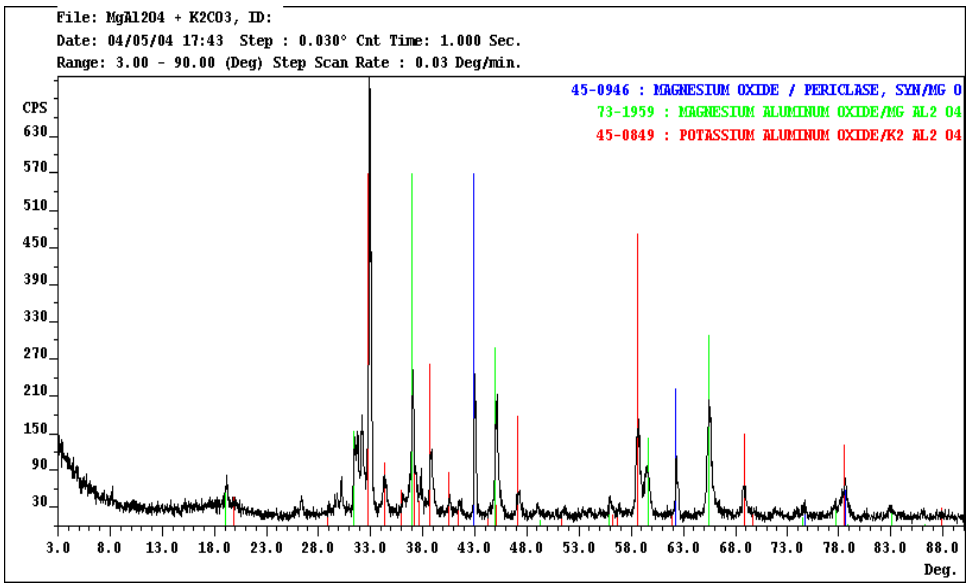

Figure 28: X-ray diffraction pattern showing reaction product potassium aluminum oxide and magnesium oxide, and original spinel

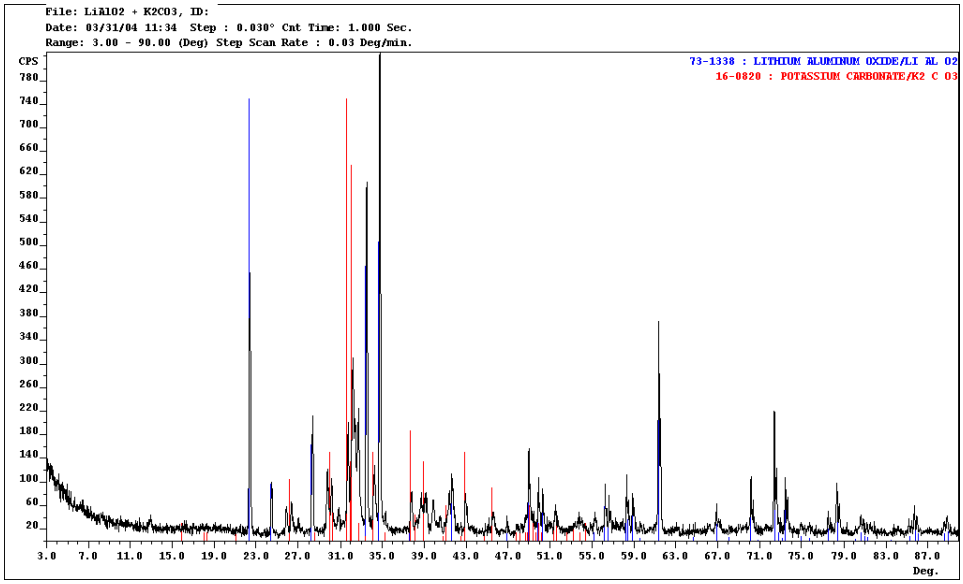

Figure 29: X-ray diffraction pattern showing lack of reaction product with original lithium aluminate and K_2CO_3 (powder mixture)

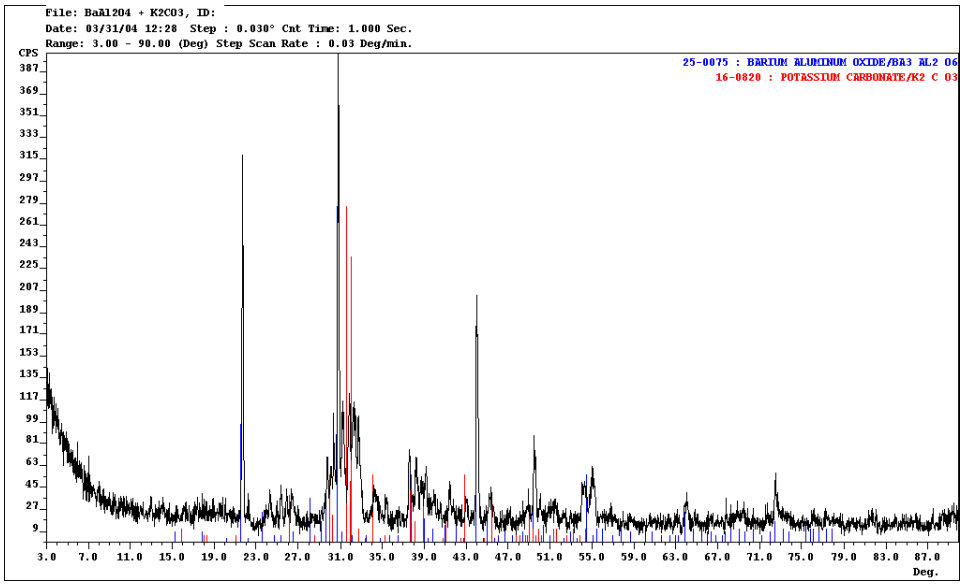

Figure 30: X-ray diffraction pattern showing lack of reaction product with original barium aluminate and K_2CO_3

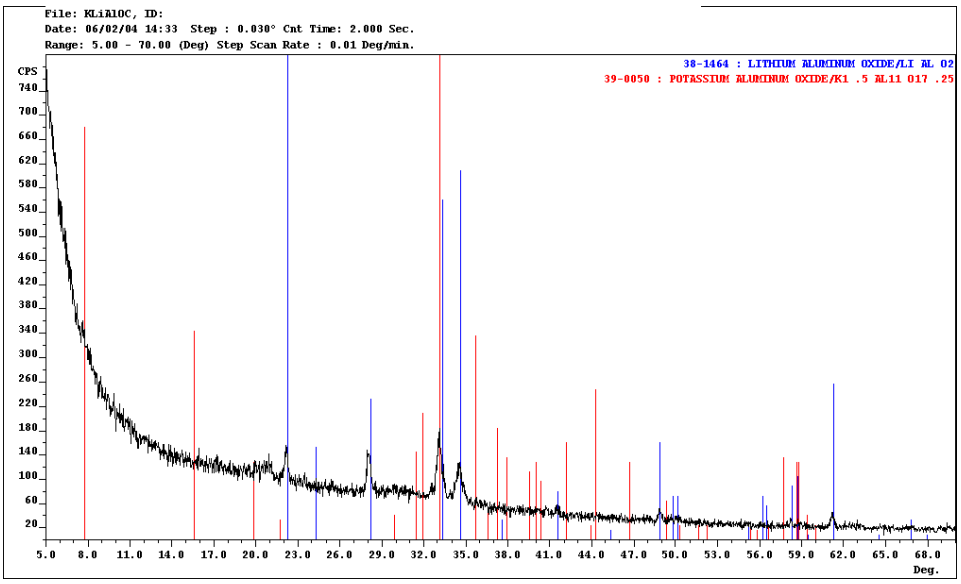

Figure 31: X-ray diffraction pattern showing reaction product of potassium aluminate with original lithium aluminate (sessile drop testing substrate)

The summary of the results from x-ray diffraction analysis of different samples is also presented in Table I and the results from thermodynamics for comparison with results of x-ray diffraction are presented in Table I.

Table I: Results of thermodynamics (FactSage) and XRD analysis at 1000°C

Candidate Material	Na_2CO_3 (Thermodynamics)	K_2CO_3 (Thermodynamics)	Na_2CO_3 (XRD)	K_2CO_3 (XRD)
Al_2O_3	X	X	X	?
$3Al_2O_3.2SiO_2$	X	X	X	?
CeO_2				
ZrO_2			X	?
MgO				
Y_2O_3			X	?
$MgAl_2O_4$		X	X	X
$LiAlO_2$ (powder mixture)				
$LiAlO_2$ (sessile drop test)			X	X
$BaAl_2O_4$ (powder mixture)			X	

(x): Reaction occurred, (?): No experiment,

Task 2.0

Considerable work has been done in the area of thermomechanical modeling of refractory linings[7-13]. Due to thermal expansion, the lining will exert pressure on itself and on surrounding materials, such as backup linings or the steel shell. Of particular interest is the behavior of the joints, these joints can potentially open up on the hot or cold face. Open joints on the hot face can cause debris or gases to condense and then penetrate the lining and cause changes in material integrity and hence its properties. The FEA method can indicate critical regions which would be unable to be seen due to dust or heat or the fact that the problem lies within the lining. Once the potential problem area has been indicated, the simulation can be used to predict the effect of changing the material, the geometry of the bricks or the geometry of the containing vessel.

Entrained flow gasifiers are generally cylindrical, range from 1.5 to 25 meters in height and 0.5 to 5 meters in diameter[14]. In the gasifier reactor vessels, there are usually 2-6 coaxial layers of component lining. The refractory lining is an integral part in the majority of gasifiers. A dense material layer is designed to be exposed to the highest temperature environment. The second layer is usually chosen with a similar material as a "safety" layer. Subsequent layers are used to provide insulation and expansion allowance, as needed. The steel shell is used to provide reaction space and confinement to the refractory lining. The temperature in the reactor would reach 950 to 1000 ^{o}C.

Because of axisymmetry, a model with half bricks would be enough for the simulation of whole cross section, Figure 32. The model is composed of two layers of refractory linings and one steel shell. Each layer of refractory lining consists of one half brick. The outer diameter of the reactor is 3 m. The thicknesses for both refractory layers are 152 mm, the

thickness of the shell is 9 mm, and there is a 1mm expansion allowance between the outer layer and the steel shell.

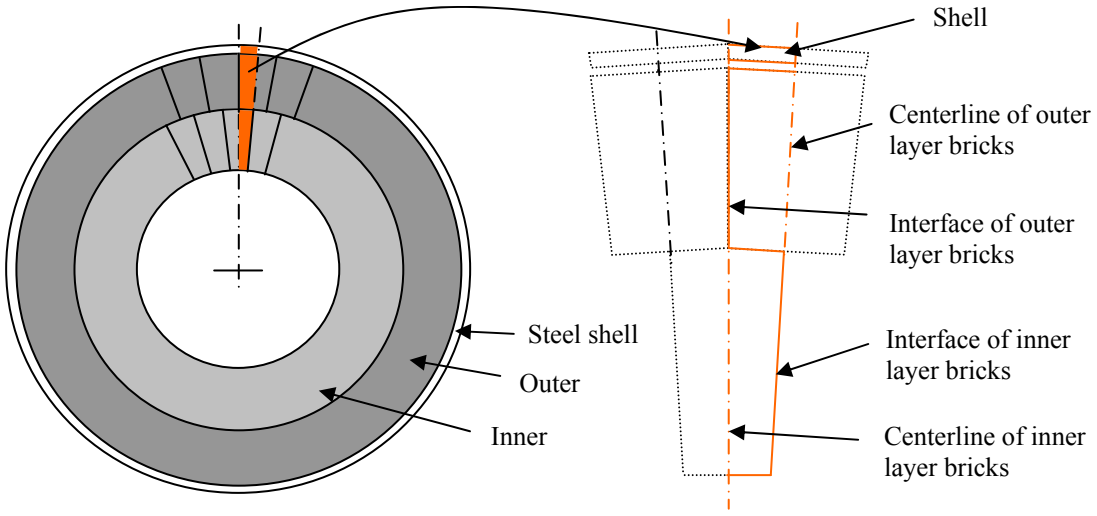

Figure 32: Illustration of the modeled part in black liquor gasifier

Heat transfer and static stress analysis were conducted in the model. The temperature distribution and history were given in the heat transfer analysis and the stress analysis gives the thermomechanical results by using the results from the heat transfer analysis. Alumina refractory is used for both inner and outer refractory layers. Carbon steel material is used for the shell. The material is assumed to be elastic-plastic. Temperature dependent material properties were used for the analysis as given in Table II[15].

Table II: Temperature dependent material properties used in the model

	Alumina, Temperature (^oC)	Steel, Temperature (^oC)
Elastic Modulus (GPa)	103, 23 81, 900	210, 23 175,400
Poisson's ration	0.20	0.3
Density (kg/m^3)	3480	7800
Coefficient of thermal expansion (1/K)	8.70E-06, 23 7.80E-06, 1450	1.3
Thermal conductivity (W/m K)	9.34, 23 9.28, 100 8.29, 200 7.55, 300 6.75, 400 5.81, 500 4.37, 600 4.65, 700 4.76, 800 4.86, 900 5.21, 1000	55,23 44,400
Specific heat (J/g K)	778, 23 916, 100 1010, 200 1080, 300 1130, 400 1170, 500 1210, 600 1220, 700 1240, 800 1250, 900 1270, 1000	500

The reactor is heated up to 950 ^oC in the model. Heat is conducted through the wall and dissipated by radiation from the outside shell surfaces to the surrounding medium which is assumed to be at a temperature of 49°C. Three different heating up rates (950^oC/h, 95^oC/h and 9.5^oC/h) were studied, as shown in Figure 33. The stress histories of these cases were compared, thereby giving the safe maximum heating rate. Then the heat transfer and thermomechanical performance were analyzed for the case with the safe maximum heating rate.

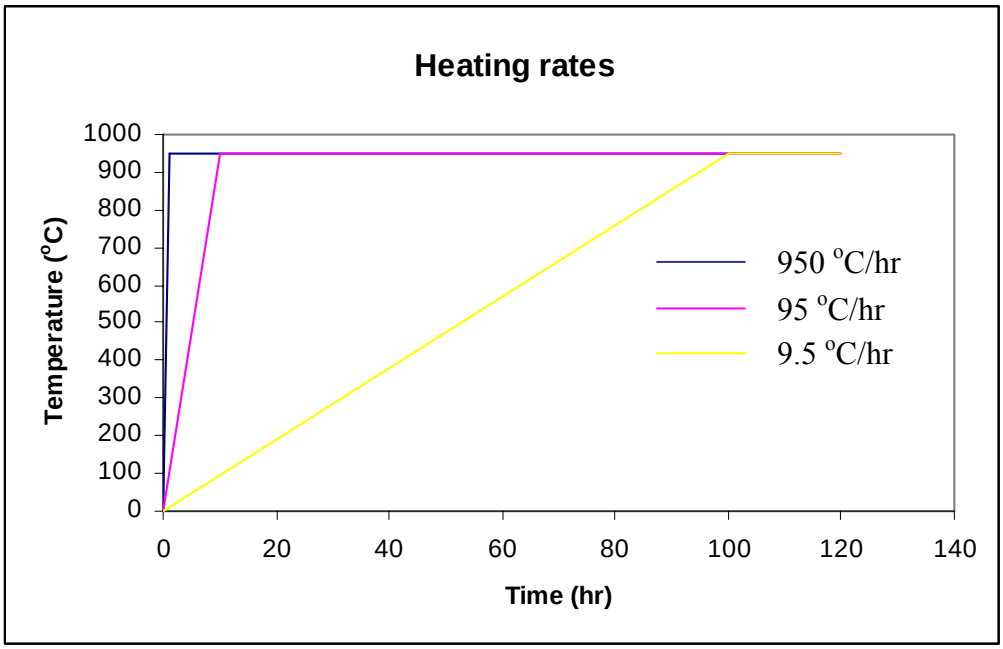

Figure 33: Heating Profile

The comparison of hoop stresses in the steel vessel at different heating rates is given in Figure 34. Heating rate doesn't affect the value of steady state stress, but it affects the peak value of the stress. In the cases with heating rates 950 °C/hour and 95 °C/hour, the highest hoop stress reaches 900 MPa and 500 MPa, respectively, the failure of the steel shell would happen under these stresses. At a heating rate 9.5 °C/hour, the peak value of the hoop stress is about 230 MPa; this is lower than the strength of steel which is about 250 MPa. So, heating rate at 9.5 °C/hour and lower is considered safe for the steel shell in the model.

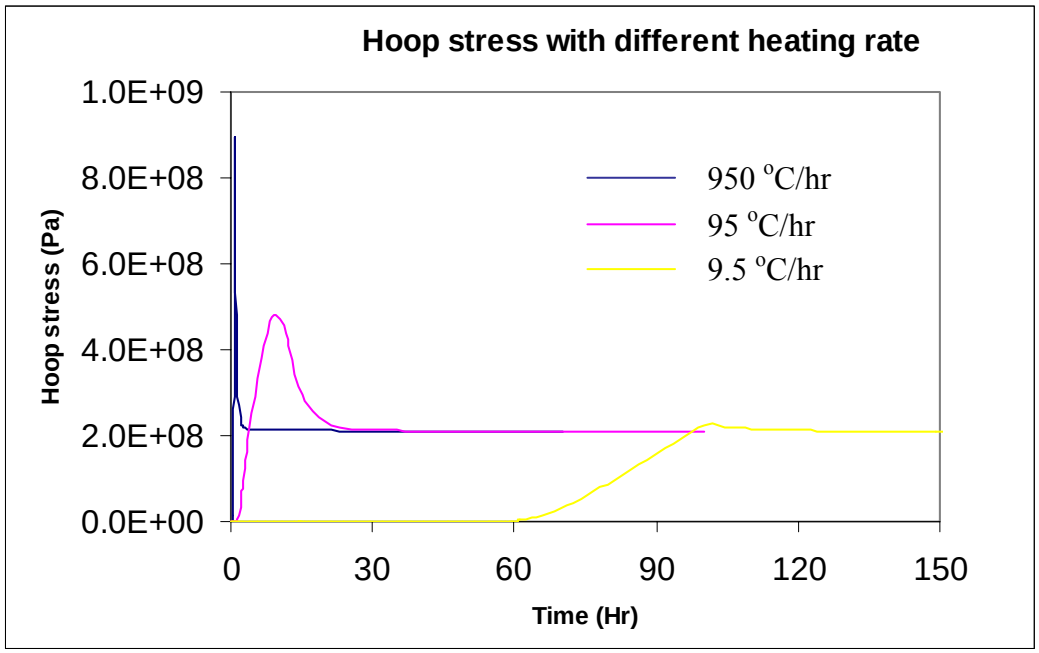

Figure 34: Hoop stress histories with different heating rates

Then heating with a rate at 9.5°C/hour was chosen for further analysis. The heat transfer and thermomechanical results are given in Figure 35.

Through thickness temperature are given in Figure 8. Temperature gradients were produced during heat up. The temperatures in the inner layer are from 650 to 950 °C, the temperatures in the outer layer are from 390 to 650 °C. Since there is no insulation between the refractory lining and the shell in the model, the temperature in the shell is close to the outer layer cold face temperature at about 385 °C. Also, because of the shell is very thin and has high thermal conductivity, the temperatures in the shell are almost within the same range. Due to very small heat conduction resistance defined between both two refractory layers and the lining and shell, there are almost no temperature gradients in the interface between two lining layers and the interface between lining and shell.

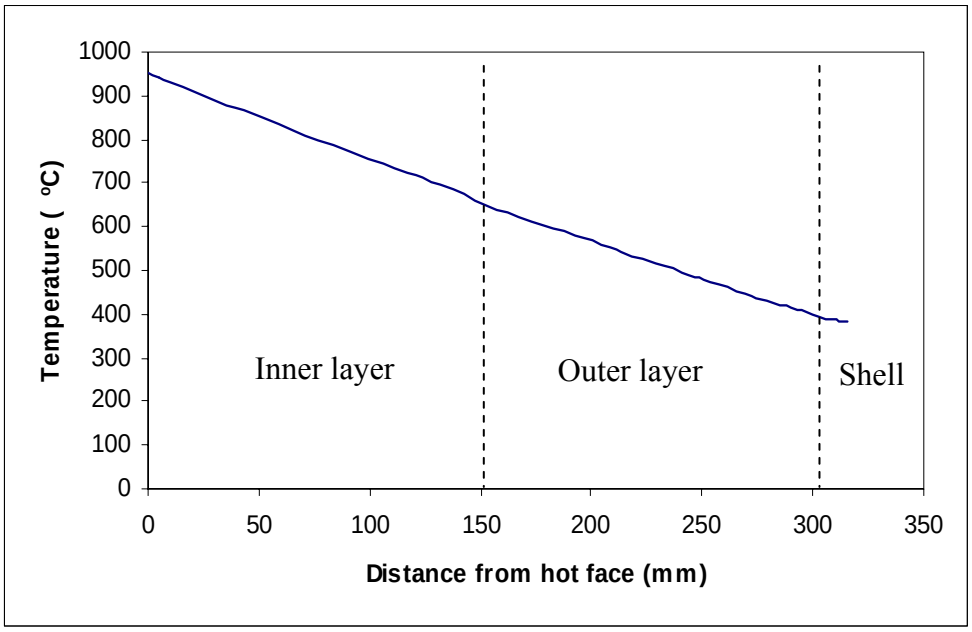

Figure 35: Through thickness temperature

Temperature gradients cause differential thermal expansion through the thickness of gasifier vessel. The thermal expansion, the interactions and confinements among the refractory layers and the steel shell produce the stresses and the strains in the gasifier reactor vessel. Combined stress, strain and temperature historical curves in the inner layer and outer layer bricks are given in Figure 36 and 37, respectively. Before the reactor is heated up to 500 ^{o}C, tensile radial stress is produced in the inner layer, then the stress turns to compressive during the rest of heat up. Compressive radial stress is produced in the outer layer lining through-out the heat up. The results also indicate that the temperature dominates the strain development. As temperature increases, the strain increases, regardless of the change in stress. Suitable heat up profile should be designed for the stability of the reactor vessel.

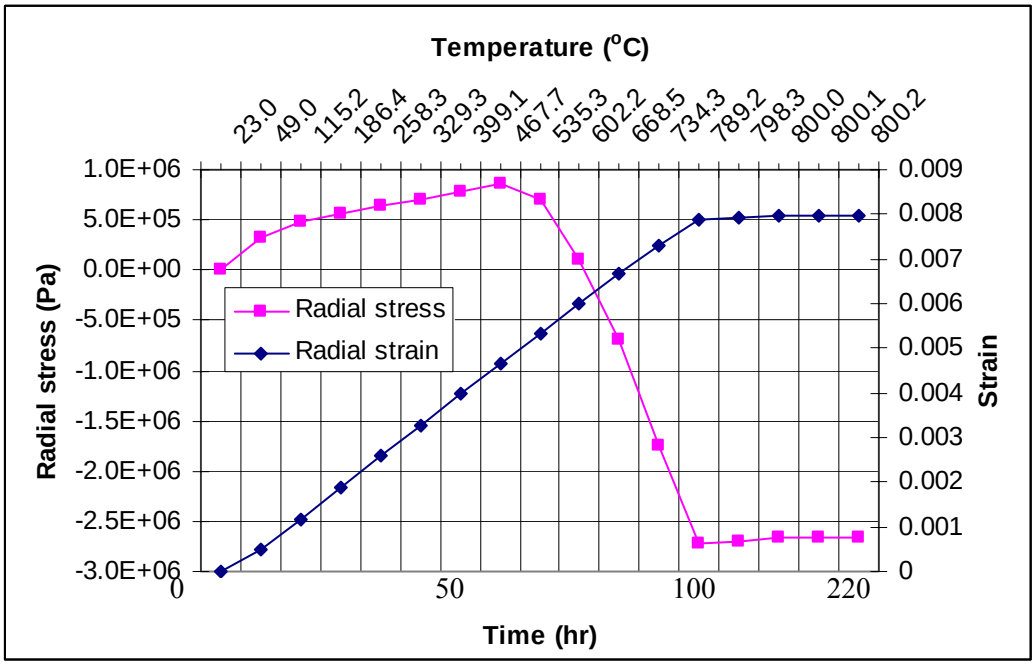

Figure 36: Stress-strain vs. temperature & time in the inner layer brick

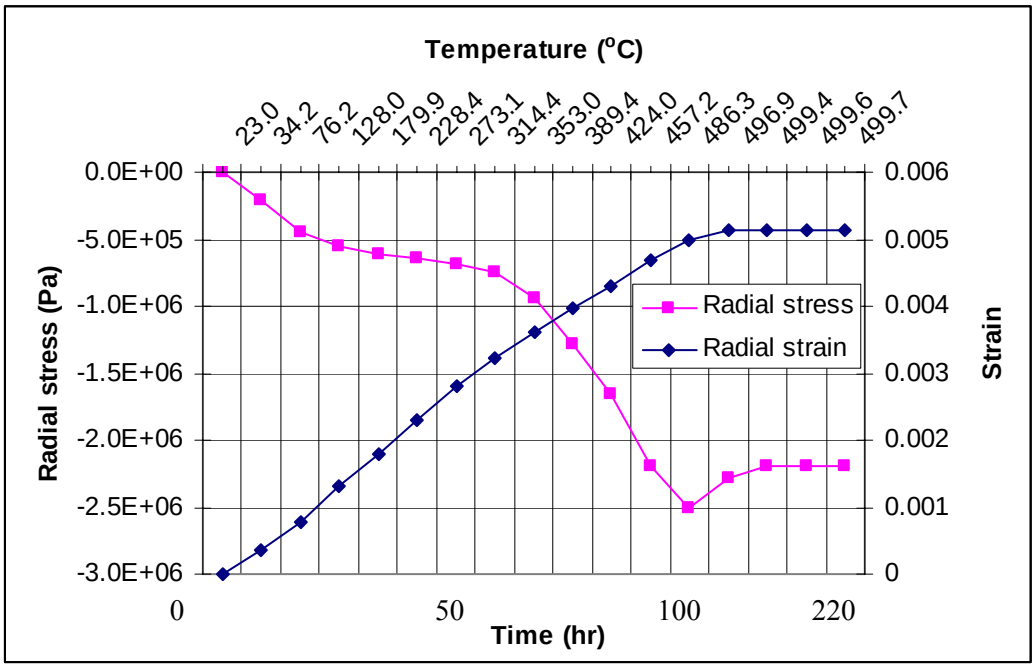

Figure 37: Stress-strain vs. temperature & time in the outer layer brick

CONCLUSION

The results of thermodynamics and experiment were in agreement for some candidate materials and were not in agreement for some. Therefore experimental work is always necessary to evaluate the materials for any application and thermodynamic predictions are not generally sufficient. So far magnesium aluminate spinel showed the highest contact angle with sodium carbonate (13 ± 1 degrees) while magnesium oxide showed the highest contact angle with potassium carbonate (10 ± 2 degrees). Although cerium oxide and magnesium oxide didn't show high contact angle with sodium carbonate and potassium carbonate but they didn't show any reaction with either one of the smelts. Therefore if a high purity material with the least amount of impurity is used for making refractory out of MgO and CeO_2 with dense microstructure, they can be promising candidates for application in black liquor gasifiers.

$MgAl_2O_4$ may still be a good candidate for BLG application although powder x-ray diffraction verified the reaction of sodium carbonate and potassium carbonate with spinel. Because sessile drop test showed relatively high contact angle with sodium carbonate and very thin reaction layer although spinel didn't have a high contact angle (3 ± 1) with potassium carbonate.

Lithium aluminate which was considered as a promising candidate before sessile drop testing doesn't seem to be an appropriate material for BLG application. Despite sessile drop testing is not sufficient for making decision about applicability of one material for this application and other experiments need to be accomplished.

A nonlinear finite element model was created for the Chemrec type gasifier reactor to simulate the operational thermomechanical environment. The heat transfer and thermomechnical results were given for the understanding of the behavior of refractory material during operational conditions.

REFERENCES

1. J. R. Keiser, R. A. Peascoe, and C. R. Hubbard, "Corrosion Issues in Black Liquor Gasifiers"; pp. 19 in Corrosion/2003 Conference Proceedings, NACE International, San Diego, CA, 2003.
2. L.L. Stigsson and B. Hesseborn, "Gasification of Black Liquor"; Section B, pp. 277-295 in International Chemical Recovery System Proceedings, Montreal Technical Section, CPPA, Toronto, Ontario, Canada, 1995.
3. L. Stigsson, "Chemrec Black Liquor Gasification"; pp. 663-674 in International Chemical Recovery Conference Proceedings, TAPPI Press, Tampa, FL, 1998.
4. C. Brown, P. Smith, N. Holmblad, G. M. Christiansen, and B. Hesseborn, "Update of North America's First Commercial Black Liquor Gasification Plant"; pp. 33-49 in Engineering and Papermakers Conference Proceedings, TAPPI Press, Nashville, TN, 1997.
5. E. D. Larson and D. R. Raymond, "Commercializing Black Liquor and Biomass Gasifier/Gas Turbine Technology," *TAPPI J.*, **80** [2], 50-57 (1997).
6. BLG project annual report, 2003.
7. Xiaoting Liang, "Modeling of Thermomechanical, Cracking and Creep Behavior in Glasstank Crown," MS Thesis, University of Missouri-Rolla, 2003
8. J. Sweeney and M. Cross, "Analyzing the Stress Response of Commercial Refractory Structures in Service at High Temperatures, II. A Thermal Stress Model for Refractory Structures," Trans. J. Br. Ceram. Soc., 81, 47-52, 1982
9. Oral Buyukozturk and Tsi-Ming Tseng, "Thermomechanical Behavior of Refractory Concrete Lining," Journal of the American Ceramic Society, 65[6] 301-307,1982
10. J. Rawers, J. Kwong, and J. Bennett, "Characterizing Coal-gasifier Slag-refractory Interactions," Materials at High Temperatures, 16[4] 219-222, 1999
11. EnSheng Chen, "Simulation of The Thermomechanical Behavior of Monolithic Refractory Lining in Coal Gasification Environment," Radex Rundschau, 4, 376-384, 1990
12. K. Andreev, H. Harmuth, "FEM Simulation of The Thermo-mechanical Behaviour and Failure of Refractories - A Case Study," Journal of Materials Processing Technology, 143-144[1] 72-77, 2003
13. Suat Yilmaz, "Thermomechanical Modeling for Refractory Lining of a Steel Ladle Lifted by Crane," Steel Research, 74[8] 485-490, 2003
14. Wade A. Taber, "Refractories for Gasification," Refractories Applications and News, 8[4] 18-22, 2003
15. J. G. Hemrick, "Creep Behavior and Physical Characterization of Fusion-Cast Alumina Refractories", PhD Dissertation, University of Missouri-Rolla, 2001

BIBLIOGRAPHY

W. E. Lee, S. Zhang, "Melt Corrosion of Oxide and Oxide-Carbon Refractories", A Review from Dept. of Engineering Materials, University of Sheffield, UK., 1999.
V. G. Levich, "Physicochemical Hydrodyanamics", 1962. Englewood Cliffs, NJ, USA, Prentice-Hall.
W. D. Kingery, H. K. Bowen, D. R. Uhlmann, "Introduction to Ceramics", Second ed. , John Wiley & Sons. New York, 1976.
R. A. McCauley, "Corrosion of Ceramics", 1994, New York, Marcel Deker.
M. L. Millard, "The Effect of Microstructure on the Liquid Corrosion of Sodium Chloride and Aluminum Oxide", Ph.D. Dissertation, Department of Ceramic Engineering, University of Missouri-Rolla, 1982.
Y. Chung, "Corrosion of Partially Stabilized Zirconia by Steelmaking Slags", M.S. Thesis, Department of Ceramic Engineering, University of Missouri-Rolla, 1993.
C. Wagner, "The Dissolution Rate of Sodium Chloride with Diffusion and Natural Convection as Rate-Determining Factors", J. Phys. Colloid Chem., 53, 1030-33, 1949.
L. Reed, L. R. Barrett, "The Slagging of Refractories, I. The Controlling Mechanism in Refractory Corrosion", Trans. Brit. Ceram. Soc, 54, 671-676, 1955.
Y. Kuromitsu, H. Yoshida, "Interaction between Alumina and Binary Glasses", J. Am. Ceram. Soc, 80 [6] 1583-87, 1997.
L. Reed, L. R. Barrett, "The Slagging of Refractories, II. The Kinetics of Corrosion", Trans. Brit. Ceram. Soc. 63, 509-534, 1964.
R. Sangiorgi, "Corrosion of Ceramics by Liquid Metals", NATO ASI Ser., Ser E., Applied Sciences, Vol. 267, pp. 261-84, 1994
N. McCallum, L. R. Barrett, "Some Aspects of the Corrosion of Refractories", Trans. Brit. Ceram. Soc., 51, 523-543, 1952.
A. R. Cooper, Jr, W. D. Kingery, "Dissolution in Ceramic Systems: I, Molecular Diffusion, Natural Convection and Forced Studies of Sapphire Dissolution in Calcium Aluminum Silicate", J. Am. Ceram. Soc, 47 [1], 37- 43, 1964.
M. P. Borom, R. H. Arendt, "Dissolution of Oxides of Y, Al, Mg, and La by Molten Fluorides", Ceramic Bulletin, 60 [11], 1169-1174, 1981.
S. E. Feldman, W. K. Lu, "Kinetics of the Reactions between Silica and Alumino-Silicate Refractories and Molten Iron", Metallurgical Transactions, 5, 249-253, 1974.
B. N. Samaddar, W. D. Kingery, A. R. Cooper, "Dissolution in Ceramic Systems: II, Dissolution of Alumina, Mullite, Anorthite, and Silica in a Calcium-Aluminum-Silicate Slag", J. Am. Ceram. Soc, 47 [5] 249-254.
K. McAlister & E. Wolfe, "A Study of the Effects of Alkali Attack on Refractories Used in Incineration", Proceedings of Incineration Conference, Albuquerque, New Mexico, pp.631-638 (1992).
Yamaguchi, A, "Reactions between Alkaline Vapors and Refractories for Glass Tank Furnaces", Proceedings of International Congress on Glass, Kyoto, Japan, pp.1-8 (1974).
Thomas, Everett A, "A Study of Soda and Potash Vapor Attack on Super Structure Refractories", *J. Can. Ceram. Soc*, **44**, 37-41 (1975).
Brown, N.R. "Alkali Vapor Attack of Alumino-Silicate refractories", Proceedings of International Ceramic Conference: AUSTCERAM 88, Sydney, pp.711-715, (1988).

Kennedy, Christophere R, "Alkali attack on mullite refractory in the grand forks energy technology center slagging gasifier", *Journal of Materials for Energy Systems*, **3**[N-1, June] 27-31, (1981).
LeBlanc, John R, "Brockway's Lower Checker Sulfate Test", *J. Can. Ceram. Society*, **52**, 58-60, (1983).
Barrie H. Bieler, "Corrosion of AZS, Zircon and Silica Refractories by Vapors of NaOH and of Na_2CO_3", *J. Am. Ceram. Soc. Bull*, **61**[7], 745-749, (1982).
R. A. Peascoe, J. R. Keiser, "Performance of Selected Materials in Molten Alkali Salts", 10th International Symposium on Corrosion in the Pulp and Paper Industry (10th ISCPPI); Marina Congress Center, Helsinki, Finland, pp189-200, 2001.
Tadaoki Fukui, "Corrosion of Zircon Refractories by Vapors of Sodium Compounds", *Ashi Gavasu Kenkya Hokoku*, **17**(2), 77-98 (1967).
J. Gullichsen, H. Paulapuro, "Chemical Pulping, Paper Making Science and Technology", Book 6B.
J. E. Lazaroff and P. D. Ownby, "Wetting in an Electric Packaging Ceramic System: I, Wetting of Tungsten by Glass in Controlled Oxygen Partial Pressure Atmospheres," J. Am. Ceram. Soc., **78** [3] 539-44 (1995).
D. A. Weirauch Jr, J. E. Lazaroff and P. D. Ownby, "Wetting in an Electric Packaging Ceramic System: II, Wetting of Alumina by a Silicate Glass Melt under Controlled PO_2 conditions," J. Am. Ceram. Soc., **78** [11] 2923-28 (1995).
P. D. Ownby, Ke Wen K. Li, D. A. Weirauch Jr, "High Temperature Wetting of Sapphire by Aluminum," J. Am. Ceram. Soc., **74** [6] 1275-81 (1991).
James Cantrell, P.E., "Simulation of Kraft Black Liquor Gasification – A Comparative Look at Performance and Economics", Engineering/Fishing & Converting Conference & Trade Fair, 1181-1195, 2001
Gupta Abha, Rajan Nidhi, Mathur R.M. and Kulkarni A.G., "Development of Lignin By-Products for Industrial Applications", IPPTA Convention, 13, 49-55, 2001
Mikael Ahlroth, Gunnar Svedberg, "Case Study on Simultaneous Gasification of Black Liquor and Biomass in a Pulp Mill," International Gas Turbine & Aeroengine Congress & Exhibition, 1998
Eric D. Larson, Stefano Consonni, and Ryan E. Katofsky, "A Cost-Benefit Assessment of Biomass Gasification Power Generation in the Pulp and Paper Industry," Final report, Princeton Unversity, Navigant Consulting, Inc., and Dipartimento di Energetica, 2003
E. G. Kelleher and A. L. Kohl, "Black Liquor Gasification Technology", Presented at the 1986 Summer National Meeting, American Institute of Chemical Engineers, August 24-28, 1986
Keijo Salmenoja, "Black-Liquor Gasification: Theoretical and Experimental Studies,", Bioresource Technology, 46, 167-171, 1993
Kirk J. Finchem, "Black Liquor Gasification Research Yields Recovery Options for Future", 69[11] 51-59, 1995
Eric D. Larson and Delmar R. Rqymond, "Commercializing Black Liquor and Biomass Gasifier/Gas Turbine Technology", TAPPI Journal, 50 – 57, 1997
Ken Patrick, "Gasification Edges Closer to Commercial Readily with Three N.A. Mill Startups", PaperAge, 30-33, 2003

Craig A. Brown and W. Densmore Hunter, "Operating Experience at North America's First Commercial Black Liquor Gasification Plant", International Chemical Recovery Conference, 655-662, 1998
J. A. Dickinson, C. L. Verrill and J. B. Kitto, "Development and Evaluation of a Low-Temperature Gasification Process for Chemical Recovery from Kraft Black Liquor," International Chemical Recovery Conference, June 1-4, 1998
Lars Stigsson, "ChemrecTM Black Liquor Gasification," International Chemical Recovery Conference, 663-674, 1998
Magnus Marklund, "Black Liquor Recovery: How Does It Work?" ETC, (Energy Technology Center, Sweden, http://www.etcpitea.se/blg/document/PBLG_or_RB.pdf
Ayhan Demirbas, "Pyrolysis and Steam Gasification Processes of Black Liquor," Energy Conversion and Management, 43, 877-884, 2002
Terry N. Adams, "Black Liquor Properties, Crystallization, and Sodium Salt Scaling in Concentrators," TAPPI 2001 Pulping Conference, 1209-1222, 2001
"Gasification of Solid and Liquid Fuels for Power Generation", Technology status report to Department of Trade and Industry, 1998,
http://www.dti.gov.uk/energy/coal/cfft/cct/pub/tsr008.pdf
Shigekastu Mori et. al., "Gasification Process of Organic Wastes for Electric Power Generation by Fuel Cell",
http://www.cape.canterbury.ac.nz/Apcche_Proceedings/APCChE/Data/720REV.pdf
Alexander Klein, "Gasification: An Alternative Process for Energy Recovery and Disposal of Municipal Solid Wastes", Master Thesis, Columbia University, 2002,
"Coal Gasification for Power Generation",
http://www.dti.gov.uk/energy/developep/chevron_texaco_part2.pdf
Kenneth T. Hood and Gunnar B. Henningsen, "Black Liquor Gasification…Evaluation of Past Experience in order to Define the Roadmap of the Future Pathway", TAPPI Fall Conference & Trade Fair, 1451-1463, 2002
Dave G. Newport, Lee N. Rockvam and Robert S. Rowbottom, "Leading Paper-Black Liquor Steam Reformer Start-up at Norampac," Presented at 2004 International Chemical Recovery Conference, Charleston, SC, June, 2004
Brown, C., Landalv, I., "The Chemrec Black Liquor Recovery Technology – A Status Report," 2001 International Chemical Recovery Conference, Whistler, B.C., 2001
Craig A. Brown, Ray Leary, J. Peter Gorog and Zia Abdullah, "The Chemrec Black Liquor Gasifier at New Bern – A Status Report," 2004 International Chemical Recovery Conference, 1089- 1093, 2004
Robert A. Peascoe, James R. Keiser, Camden R. Hubbard, Michael P. Brady and J. Peter Gorog, "Performance of selected materials in molten alkali salts," International Symposium on Corrosion in the Pulp & Paper Industry 2001, 189-200, 2001
Roberta A. Peascoe, James R. Keiser, Camden R. Hubbard, J. Peter Gorog, Craig A. Brown and Bengt H. Nilsson, "Comparison of Refractory Performance in Black Liquor Gasifiers and A Smelt Test System," 2001 International Chemical Recovery Conference, Whistler, B.C., 2001
Xiaoting Liang, "Modeling of Thermomechanical, Cracking and Creep Behavior in Glasstank Crown," MS Thesis, University of Missouri-Rolla, 2003

J. Sweeney and M. Cross, “Analyzing the Stress Response of Commercial Refractory Structures in Service at High Temperatures, II. A Thermal Stress Model for Refractory Structures,” Trans. J. Br. Ceram. Soc., 81, 47-52, 1982
Oral Buyukozturk and Tsi-Ming Tseng, “Thermomechanical Behavior of Refractory Concrete Lining,” Journal of the American Ceramic Society, 65[6] 301-307,1982
J. Rawers, J. Kwong, and J. Bennett, “Characterizing Coal-gasifier Slag-refractory Interactions,” Materials at High Temperatures, 16[4] 219-222, 1999
EnSheng Chen, “Simulation of The Thermomechanical Behavior of Monolithic Refractory Lining in Coal Gasification Environment,” Radex Rundschau, 4, 376-384, 1990
K. Andreev, H. Harmuth, “FEM Simulation of The Thermo-mechanical Behaviour and Failure of Refractories - A Case Study,” Journal of Materials Processing Technology, 143-144[1] 72-77, 2003
Suat Yilmaz, “Thermomechanical Modeling for Refractory Lining of a Steel Ladle Lifted by Crane,” Steel Research, 74[8] 485-490, 2003
Wade A. Taber, “Refractories for Gasification,” Refractories Applications and News, 8[4] 18-22, 2003
J. G. Hemrick, “Creep Behavior and Physical Characterization of Fusion-Cast Alumina Refractories”, PhD Dissertation, University of Missouri-Rolla, 2001

LIST OF ACRONYMS AND ABBREVIATIONS

BLG=Black Liquor Gasification
LPLT=Low Pressure Low Temperature
HPLT=High Pressure Low Temperature
LPHT=Low Pressure High Temperature
HPHT=High Pressure High Temperature
T_m=melting point temperatura
SEM=Scanning Electrón Microscope
EDS=Energy Dispersive Spectroscopy
XRD=X-Ray Diffraction
T=Temperature